University of New Hampshire
University of New Hampshire Scholars' Repository

Honors Theses and Capstones | Student Scholarship

Spring 2021

Roles of Non-Frankia Bacteria in Root Nodule Formation and Function in Alnus sp.

Kelsey Christine Mercurio
University of New Hampshire, Durham

Follow this and additional works at: https://scholars.unh.edu/honors

 Part of the Agriculture Commons, Biology Commons, Environmental Microbiology and Microbial Ecology Commons, Microbial Physiology Commons, and the Plant Biology Commons

Recommended Citation

Mercurio, Kelsey Christine, "Roles of Non-Frankia Bacteria in Root Nodule Formation and Function in Alnus sp." (2021). *Honors Theses and Capstones*. 603.
https://scholars.unh.edu/honors/603

This Senior Honors Thesis is brought to you for free and open access by the Student Scholarship at University of New Hampshire Scholars' Repository. It has been accepted for inclusion in Honors Theses and Capstones by an authorized administrator of University of New Hampshire Scholars' Repository. For more information, please contact Scholarly.Communication@unh.edu.

Roles of Non-*Frankia* Bacteria in Root Nodule Formation and Function in *Alnus* sp.

Honors Senior Thesis, University of New Hampshire,
Kelsey Mercurio

Additional Contributors: Céline Pesce, Ian Davis, Erik Swanson, Lilly Friedman, & Louis S. Tisa

Department of Molecular, Cellular, and Biomedical Sciences
University of New Hampshire, Durham, NH, USA.

Roles of non-*Frankia* bacteria in root nodule formation and function in *Alnus* sp.

Abstract:
Plant roots are home to a wide variety of beneficial microbes; understanding and optimizing plant-microbe interactions may be critical to enhance global food security in a sustainable, equitable way. With the help of their nitrogen-fixing bacterial partner, *Frankia*, actinorhizal plants form symbiotic root nodules and play important roles in agroforestry and land reclamation. However, *Frankia* does not live alone in nodules, and the other microbial residents may contribute to nodule formation and function. We collected root nodules from alder trees (*Alnus* sp.) in 2018 and 2019, then isolated DNA and individual bacterial strains to characterize the nodule microbial community. Of 88 isolates, several were identified via 16S amplicon sequencing, and we chose ten isolates for whole genome sequencing. To test effects on the host plant, we used four isolates to inoculate sterile *Alnus glutinosa* plants, both alone and in co-culture with Frankia. Nodule formation and plant growth and health were monitored under nitrogen-deficient conditions. We also tested several isolates for plant-growth-promoting properties including auxin production, siderophore production, and phosphate solubilizing ability. *Thiopseudomonas* sp. (strain 21), strain 85J, *Streptomyces* (24), and *Paenibacillus* (61) increased plant chlorophyll content in co-inoculation with *Frankia*, and strain 85J produced pseudonodules in the absence of Frankia. Multiple strains produced the auxins indole-3-butyric acid (12, 61), indole-3-acetic acid (17, 24), or both (9, 21, 70, 76), and enzymes associated with IAA production could be identified in the genomes of strains 12, 17, 24, and 9. On exposure to root exudates from nitrogen-stressed plants, *Bacillus* sp. (76) produced less indole-3-butyric acid and more indole-3-acetic acid, possibly indicating activation of a signaling pathway or regulatory response. Additionally, multiple strains produced siderophores (10, 12, 34, 69, 81, 88, 88A, 98) and/or solubilized phosphate (9, 30, 34, 55, 69, 81). Overall, non-*Frankia* bacteria living in alder nodules appear to play specific roles in plant health, nodule formation, and nodule function. Understanding how nodules function as a community rather than simply a two-way interaction can help us optimize nitrogen fixation and inform our use of actinorhizal and legume plants in agriculture and bioremediation.

Introduction:

Plant roots are home to a wide variety of beneficial microbes. Given the ability of microorganisms to help plants obtain nutrients, tolerate biotic and abiotic stress, and sustain growth without the energy or pollution costs associated with certain agricultural inputs (Kumar et al. 2018), understanding and optimizing plant-microbe interactions may be critical to enhance global food security in a sustainable, equitable way. While many studies focus on understanding crop-associated microbial communities and specific beneficial interactions, microorganisms that support non-crop plants may be just as crucial in designing sustainable agricultural systems. Particularly, bacteria and fungi that associate with cover crops and woody intercrops play important roles in nutrient transformation and storage, improving soil water-holding capacity, and bioremediation, either directly or through their support of plant processes. (Castellano-Hinojosa & Strauss 2020, Ingleby et al. 2007, Ngom et al. 2016; Bhadha et al. 2017). Plant-associated microorganisms also play essential roles in natural ecosystems, for example by helping early succession plants colonize harsh environments (Gagnon et al. 2020).

Actinorhizal plants are dicotyledons, typically woody, that come from eight families and are defined by their ability to form symbiotic root nodules with members of *Frankia*, a genus of nitrogen-fixing actinobacteria, (Diagne et al. 2013). Actinorhizal plants are used in land reclamation efforts due to their ability to improve soil quality, control erosion, and tolerate and/or remove contaminants like heavy metals and excess salt (Diagne et al. 2015, Gagne et al. 2020). Some species also play a role in integrated agroforestry systems for their nitrogen contributions and production of products such as firewood and

medicinal compounds, as in Papua New Guinea (Bourke 1985), India (Saravanan ad Vijayaraghavan 2014), Costa Rica (Dommergues), and Peru (A. Ogden, personal communication). Although genetic and genomic tools in both *Frankia* and their plant partners have been improving, the actinorhizal symbiosis is not as well characterized as compared to the agriculturally important legume-rhizobia symbiosis (Cissoko et al. 2018 , Franche & Bogusz 2011).

Like in the legume-rhizobia symbiosis, nodule formation in actinorhizal plants with *Frankia* begins with an exchange of signals. Infection can occur either intracellularly (inside plant cells), as in *Alnus*, *Myrica*, *Comptonia*, *Casuarina,* and *Gymnostoma*, or intercellularly (between plant cells), as in various genera in the families Eleagnaceae, Rhamnaceae, Rosaceae, Datiscaceae and Coriariaceae, though intracellular infection eventually occurs in both processes (Franche & Bogusz 2011). In the intracellular process, host plant roots respond to nitrogen-deficient conditions by releasing flavonoids to recruit bacteria, and *Frankia* responds by releasing a hydrophilic signal that stimulates root hair deformation (Franche & Bogusz 2011, Cissoko et al. 2018). The *Frankia*-derived signal have been partially characterized as NIN-activating factor (CgNINA) in the symbiont of *Casuarina glauca* and root hair deforming factor (AgRHDF) in the symbiont of *Alnus glutinosa*. Although structures for these signals have not yet been determined, they differ from the Nod signals produced by rhizobia in that they are hydrophilic and cannot be destroyed with chitinase (Cissoko et al. 2018). *Frankia* hyphae penetrate the curling root hair, encapsulated by plant-derived polygalacturonans and plasma membrane, and begin dividing within root cortical cells (which also divide), forming a “prenodule” that is thought to be an ancestral symbiotic organ (Franche & Bogusz 2011). Meanwhile, the plant activates another signal cascade that is thought to connect to the common symbiotic pathway used in mycorrhizal and rhizobia symbioses (Franche & Bogusz 2011). The hyphae continue until they reach the pericycle, a layer of stem cells in the stele that can differentiate into secondary roots (Franche & Bogusz 2011), forming a nodule primordium. The nodule primordium develops into a fully functioning nitrogen-fixing root nodule, which branches into lobes due to its association with secondary roots (Franche & Bogusz 2011).

Although signaling studies understandably focus on *Frankia*, research on the microbiome of several actinorhizal plants has revealed that *Frankia* is typically not the only bacterial inhabitant of the nodules, and the roles of these other bacteria are poorly understood (D’Angelo et al. 2016, Valdés et al. 2005). In some environments, *Frankia* can make up as little as 0.5% of the total nodule community by chromosome copy, though this is an extreme case (D’Angelo et al. 2016). In legumes, so-called nodule “helper” bacteria have been found to increase nitrogen fixation and modulate the number, size, and composition of root nodules (Soe et al. 2012, Soe & Yamakawa 2013, Gregor et al. 2003, Tokala et al 2002, Tokala 2004, Janati et al. 2021). For example, *Streptomyces kanamycetius* selected for antibiotic-resistant rhizobia strains by producing kanamycin and neomycin in nodules, with apparent effects on nodule efficacy (Gregor et al. 2003). The hydroxamate siderophore-producing *Streptomyces lydicus* WYEC8 preferentially colonized nodules and increased nodule occupancy and health, nitrogenase activity, nodule iron and molybdenum concentrations, number of nodules, and plant growth (Tokala 2004, Tokala et al. 2002). Phosphate-solubilizing strains of *Bacillus* and/or *Pseudomonas* have been associated with enhanced nodulation and/or growth in chickpea, faba bean (*Vigna faba*), and lablab bean (*Lablab purpureus*) (Janati et al. 2021). Both iron and phosphorus play essential roles in the nitrogenase enzyme as well as in overall bacterial and plant metabolism.

In the actinorhizal symbiosis, nodule-associated non-*Frankia* bacteria may have roles similar to those of helper bacteria in legumes – for example, co-inoculation of *Alnus rubra* with *Pseudomonas cepacia* and *Frankia* approximately doubled the number of nodules compared to *Frankia* alone

(Knowlton & Dawson 1983, Knowlton et al. 1980). However, some actinobacteria strains appear to have additional roles that mirror *Frankia*. Non-*Frankia* actinobacteria, including *Micromonospora* strain L5, isolated from *Casuarina equestifolia* nodules in Mexico appear to fix nitrogen based on the presence of amplified nif genes, ability to grow in nitrogen-free medium, and ability to incorporate $^{15}N_2$ (Valdés et al. 2005). Two *Norcardia* isolates from nodules of *Casuarina glauca* induce root hair deformation, produce nodule-like structures ("pseudonodules") on the host plant, promote plant growth, and produce low levels of the auxin indole butyric acid (IBA) (Ghodhbane-Gtari et al. 2019). Strain BMG111209 additionally activates the NIN promoter associated with nodulation, and strain BMG51109 produces the auxins indole acetic acid (IAA) and phenylacetic acid (PAA), which are also produced by *Frankia* and are important for differentiation of *Frankia*-infected plant cells (Ghodhbane-Gtari et al. 2019, Perrine-Walker et al. 2010, Péret et al. 2007).

In this study, we aimed to characterize the culturable nodule community of alders (*Alnus incana* or *A. serrulata*) from a coastal wetland in New Hampshire & understand the roles of particular isolates in nodule function. Specifically, the study focused on isolation of bacteria from nodules, screening isolates for traits associated with plant growth promotion, and evaluating the effects of select isolates on plant growth, health, and nodulation. The study is part of a larger project that analyzes the alder nodule microbiome using a multi-faceted approach that includes microbial isolation and identification, plant and microbial physiological studies, full-genome sequencing of select strains, and culture-independent analysis of the nodule and rhizosphere bacterial communities using next-generation sequencing. Of the non-*Frankia* bacterial isolates published previously (Davis et al. 2020) as well as several new isolates, we identified eight siderophore producers, six phosphate solubilizers, and eight producers of indole-related compounds such as IAA and IBA, including members of the genera *Herbaspirillum, Rhodococcus, Kocuria, Streptomyces, Paenibacillus, Thiopseudomonas,* and *Bacillus*. The *Bacillus* appeared to switch from IBA production to IAA production on exposure to root exudates from nitrogen-stressed *Alnus glutinosa*. Additionally, *Thiopseudomonas, Streptomyces, Paenibacillus*, and strain 85J increased chlorophyll content of *A. glutinosa* leaves when co-inoculated with *Frankia* QA3, and strain 85J produced pseudonodules in the absence of *Frankia*. Understanding the alder nodule microbiome could provide vital insights into the nature of the *Frankia*-actinorhizal symbiosis, which appears to be influenced by many organisms besides *Frankia* and their host plants. Non-*Frankia* bacteria may play important roles in the ability of actinorhizal plants to withstand stress, obtain nutrients, and contribute nitrogen and organic matter to natural and agricultural ecosystems.

Methods

Nodule collection, bacterial isolation, and growth conditions

Nodulated roots were collected from three individual *Alnus* trees (either *Alnus incana* or *A. serrulata*) located near the edge of a small pond at Adam's Point in Durham, New Hampshire (Fig. 1) on September 3 and November 7, 2019. Nodules from each tree were then excised from roots and sonicated twice in sterile deionized water using a water bath at room temperature, and the resulting soil slurry was frozen at -20°C for characterization of the rhizosphere community. Nodules were surface sterilized with 30% hydrogen peroxide 60-75 minutes and rinsed thoroughly, and a subset was stored at -20°C for community DNA extraction. The remaining nodules were finely chopped under aseptic conditions, suspended in 1 mL sterile deionized water, and plated from 10^0 to 10^{-3} dilutions on the following medias with 1.5% agar: Czapek + yeast extract (per 1 L: 4 g yeast extract, 15 g sucrose, 2 g $NaNO_3$, 0.01g $FeSO_4$ x 7 H_2O, 0.5 g K_2HPO_4, 0.5 g KCl, 0.5 g $MgSO_4$ x 7 H_2O), R2A (per 1 L: 0.6 g yeast extract, 0.5 g protease peptone, 0.5 g casamino acid, 0.5 g dextrose, 0.5 g soluble starch, 0.3 g sodium

pyruvate, 0.05 g $MgSO_4$ x 7 H_2O), and either MPN mm^- in September (per 1 L: 14.7 g MOPS buffer, 5.95 g K_2HPO_4, 0.94 g NH_4Cl) or MPN 10:10:5 in November (per 1 L: MPN + 10 mM glucose, 10 mM sodium succinate, 5 mM sodium propionate, metals mix – see appendix). After incubation at 28°C ranging from a few days to multiple weeks, colonies were streaked for isolation and grown in liquid culture using their media of origin (or MPN 10:10:5 for colonies from MPN mm^-), and -80°C stocks were prepared by mixing equal ratios of culture and 60% glycerol.

Frankia strain QA3 was grown at 28°C in MPN with 5 mM propionate. Every few weeks the cells were harvested and sub-cultured in fresh medium, and a homogenization step was included whenever hyphae formed large clumps. Several strains isolated from the same stand of alders in spring and fall 2018 (Davis et al. 2020) were cultivated in liquid Czapek or R2A as needed, while the 2019 isolates were cultivated in Czapek or their media of origin. Strains that grew to a usable density within 1-3 days were cultivated as needed just before use, but several of the putative actinobacteria (107, 85A, 85C, 85 E, 85G, 85J) grew more slowly, and these were cultivated over several weeks with shaking and periodic homogenization and subculture.

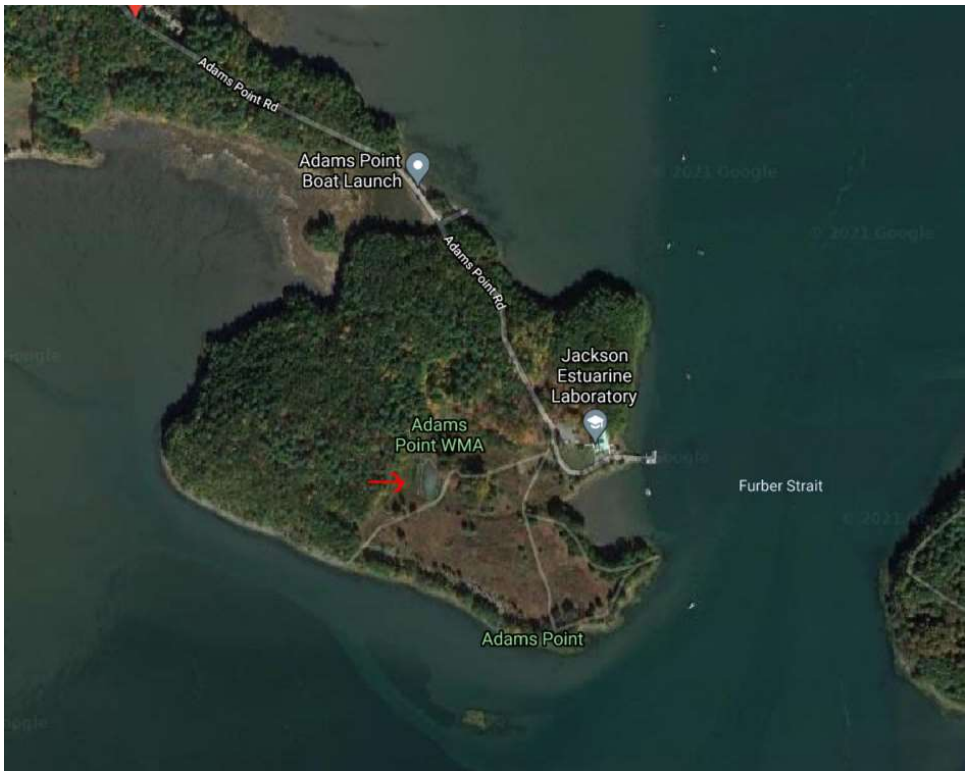

Fig. 1. Approximate location of alder stand sampled in this study, marked by red arrow (Google Maps).

Table 1. Bacterial strains isolated and/or used in various components of this study. Study components include bacterial isolation, plant inoculations, and assays to determine auxin production, siderophore production, and phosphate solubilizing ability. (Phenotypic results are not reported in this table.)

Strain	Genus	Color/ Morphology	Isolation Media	Nodule Collection Date	Source	Accession #	Study components					
							Isolation	Plant Inoculat.	Aux.	Sid	Phos. Solub.	Genomic analysis
QA3	*Frankia*	brown	N/A	N/A	Sen et al. 2013	CM001489.1		X		X	X	
DC12	*Frankia*	beige	N/A	N/A	Tisa et al. 2015	LANG00000000				X	X	
5	*Kocuria*	yellow	Czapek	May 2018	Tisa lab					X	X	
9	*Rhodococcus*	yellow-orange	R2A	May 2018					X	X	X	X
10	*Herbaspirillum*	clear	R2A	May 2018	Davis et al. 2020	ASM456392v1 SPNJ00000000				X	X	
12	*Herbaspirillum*	clear	R2A	May 2018	Davis et al. 2020	ASM456389v1 SPNI00000000			X	X	X	X
14	*Kocuria*	yellow	R2A	May 2018	Tisa lab							
16	*Kocuria*	yellow	MPN	May 2018	Tisa lab							
17	*Kocuria*	yellow	R2A	May 2018	Davis et al. 2020	ASM456377v1 SPNL00000000			X			X
21	*Thiopseudomonas*	yellow	R2A	May 2018	Davis et al. 2020	ASM456376v1 SPNM00000000		X	X	X	X	X
24	*Streptomyces*	white	R2A	May 2018	Davis et al. 2020	ASM456380v1 SPNN00000000		X	X	x	X	X
30	*Curtobacterium*	yellow	R2A	6/21/18	Tisa lab					X	X	
34	unidentified	white	R2A	6/21/18	Tisa lab					X	X	
39	*Micrococcus*	yellow	Czapek	9/20/18	Tisa lab					X	X	
41	*Bacillus*	brown	R2A	9/20/18	Tisa lab					X	X	
42	unidentified	beige	R2A	9/20/18	Tisa lab					X	X	
51	unidentified	white	Czapek	9/3/19	this study		X					
52	Staphylococcus	yellow/ beige	Czapek	9/3/19	this study		X					
53	Staphylococcus	white	Czapek	9/3/19	this study		X					
54	*Kocuria* or *Rothia*	light beige	Czapek	9/3/19	this study		X			X	X	
55	unidentified	yellow	Czapek	9/3/19	this study		X			X	X	
56	unidentified	beige	Czapek	9/3/19	this study		X					
57	unidentified	beige	Czapek	9/3/19	this study		X					
60	unidentified	beige	Czapek	9/3/19	this study		X					
61	*Paenibacillus*	clear	Czapek	9/3/19	this study		X	X	X	X	X	
67	unidentified	yellow	MPN mm-	9/3/19	this study		X					
68	unidentified	beige	MPN mm-	9/3/19	this study		X					

69	unidentified	translucent yellow	MPN mm-	9/3/19	this study		X			X	X	
70	unidentified	Dark pink or beige	MPN mm-	9/3/19	this study		X		X	X	X	
71	*Bacillus*	light beige	R2A	9/3/19	this study		X			X	X	
73	unidentified	cream	R2A	9/3/19	this study		X					
76	*Bacillus*	clear	R2A	9/3/19	this study		X	X	X	X	X	
77	*Bacillus*	translucent	R2A	9/3/19	this study		X					
81	unidentified	cream	R2A	9/3/19	this study		X			X	X	
83	unidentified	translucent	R2A	9/3/19	this study		X					
85A	unidentified	salmon hyphal	Czapek	11/7/19	this study		X					
85C	unidentified	salmon hyphal	Czapek	11/7/19	this study		X					
85E	unidentified	salmon hyphal	Czapek	11/7/19	this study		X					
85F	unidentified	salmon hyphal	Czapek	11/7/19	this study		X					
85G	unidentified	salmon hyphal	Czapek	11/7/19	this study		X			X	X	
85J	unidentified	salmon hyphal	MPN 10:10:5	11/7/19	this study		X	X	X	X	X	
85L	unidentified	salmon hyphal	MPN 10:10:5	11/7/19	this study		X			X	X	
85Q	unidentified	salmon hyphal	MPN 10:10:5	11/7/19	this study		X			X	X	
87	unidentified	cream	MPN 10:10:5	11/7/19	this study		X					
88	unidentified	cream	R2A	11/7/19	this study		X			X	X	
88A	unidentified	beige	Czapek	11/7/19	this study		X			X	X	
88B	unidentified	yellow	Czapek	11/7/19	this study		X			X	X	
91	unidentified	cream	Czapek	11/7/19	this study		X					
96	unidentified	cream	Czapek	11/7/19	this study		X					
97	unidentified	white	Czapek	11/7/19	this study		X					
98	unidentified	cream	R2A	11/7/19	this study		X			X	X	
101	unidentified	yellow	MPN 10:10:5	11/7/19	this study		X			X	X	
102	unidentified	beige	MPN 10:10:5	11/7/19	this study		X			X	X	
107	unidentified	red	MPN 10:10:5	11/7/19	this study		X					
109	unidentified	cream hyphal	MPN 10:10:5	11/7/19	this study		X					

110	unidentified	yellow	MPN 10:10:5	11/7/19	this study		X					

DNA extraction and 16S amplification

Genomic DNA (gDNA) was extracted from individual bacterial strains by the cetyltrimethylammonium bromide (CTAB) DNA extraction protocol (Murray & Thompson 1980). Briefly, bacteria were propagated from individual colonies or glycerol -80°C stocks in their media of origin (Czapek, R2A, or MPN 10:10:5) as described above. Liquid cultures were pelleted, frozen at -20°C, resuspended in 567 µL TE buffer, heated to 80°C for 30 min, and treated with 11 µL lysozyme (50 mg/mL) and 30 µL 10% sodium dodecyl sulfate (SDS) to lyse cells followed by 5 µL proteinase K (20 mg/mL). After incubation for 1 h, 100 µL 5M NaCl was added to the mixture and followed by the addition of 10% cetyl trimethyl ammonium bromide (CTAB)/0.7M NaCl. This mixture was incubated at 65°C for 10 min. An equal volume of 24:1 chloroform:isoamyl alcohol was added to the mixture. After mixing, the mixture was centrifuged for 2 min to separate the phases. The aqueous layer was removed and transferred to a new microfuge tube. DNA was precipitated by the addition of an equal volume of isopropanol. The precipitated DNA was collected by centrifugation and the supernatant fluid was discarded. The pellet was washed with cold 70% ethanol and centrifuged again. The supernatant fluid was discard and the pellet was air dried a few minutes. The pellet was resuspended in DNase-free water, and treated with RNase to remove RNA.

A subset of strains from the September isolation were identified by amplification (polymerase chain reaction) and sequencing of the conserved gene corresponding to 16S rRNA. Genomic DNA was diluted to a final mass of 100 ng per reaction and combined with 1 µL each forward and reverse primer 20 pmol/µL (20 uM) stocks (A7-26 and B1523-1504, Table 2) and 25 µL 2X HotStart Master Mix for a total volume of 50 µL. Thermocycler conditions were activation for 6 min at 96.0°C followed by 35 cycles of denaturation for 30s at 96.0°C, annealing for 30s at 70.0°C, and extension for 2 min at 68°C, followed by 5 min final extension at 68°C. PCR products were visualized on a 0.8% agarose gel, purified using a QIAquick PCR purification kit, and sent to GeneWiz for Sanger sequencing. The resulting sequences were analyzed using BLAST to assign putative genera based on alignments with 98-100% identity.
DNA was also extracted directly from nodule and rhizosphere samples to obtain community profiles. Surface-sterilized nodules stored at -20°C were crushed to powder in liquid nitrogen using a sterile mortar and pestle, which was rinsed with ethanol and water between samples. Rhizosphere suspensions were pelleted. Nodule powder or rhizosphere soil were used with a PowerSoil DNA extraction kit according to manufacturer protocol, but with final suspension of DNA in 50 µL rather than 100 µL DNAse-free water. These samples will be used for next-generation sequencing of the 16S amplicons.

Table 2. Primers used for amplification and sequencing of 16S region.

Primers	Sequence	Tm
A7-26	5’-CCG TCG ACG AGC TCA GAG TTT GAT CCT GGC TCA-3’	71.05°C
B1523-1504	5’-CCC GGG TAC CAA GCT TAA GGA GGT GAT CCA GCC GCA-3’	74.73°C
907R (sequencing, used by Genewiz)	5’-CCG TCA ATT CMT TTG AGT TT-3’	45.6-47.7°C

Aseptic plant culture

To promote germination, *Alnus glutinosa* seeds (Sheffield, Hungary) were stored for several weeks at 4°C. Prior to germination, the seeds were soaked in sterile deionized water approximately 30 hours. The soaked seeds were sterilized by incubating in 4% plant preservative mixture (Cell Tech) for 13 hours, followed by treatment with 30% hydrogen peroxide with 2 drops Tween-20 for 30 minutes. The treated seeds were thoroughly rinsing with sterile deionized water after each step. The seeds were spread in glass petri dishes containing sterile Perlite wetted with Brougton and Dilworth with nitrogen (BDN) nutrient medium (Broughton & Dilworth 1971, see appendix). After germination and appearance of the first true leaves, seedlings were transferred to Magenta GA-7 boxes containing Brite-Kote aluminum screen suspended over 50 ml of BDN, with two plants per box. The plants were incubated at 28°C with a 16 h light period for a minimum of 6 weeks, replacing the spent BDN medium every 5-6 weeks. Prior to inoculation, plants were starved of nitrogen by replacing BDN medium by BD (nitrogen-free) medium and grown for sixteen days.

Plant inoculations with *Frankia* and putative helper bacteria

Cultures of *Thiopseudomonas* (21: 4R-3D) and *Paenibacillus* (61) were grown in Czapek plus yeast extract 21.5 hours at 28°C, stored at 4°C for 27 hours, then returned to 28°C for 16 hours prior to plant inoculations. *Streptomyces* (24: 4R-3D) was grown 50 days in Czapek plus yeast extract at 28°C, then sub-cultured and homogenized 3 days prior to inoculations. Strain 85J was grown 30 days in MPN 10:10:5, then sub-cultured, homogenized, and grown an additional 24 days. *Frankia* QA3 was sub-cultured in MPN with 5 mM propionate 8 days prior to inoculation. The cells were harvested, washed twice in diluted BD medium, and resuspended in full-strength BD. Prior to inoculation, the last spent BD medium in each plant box, which contained root exudates of nitrogen-stressed alder, was removed, filtered, and stored at 4°C for use in the auxins assay. The plants were inoculated with a single bacterial strain alone or in co-inoculation with *Frankia* sp. strain QA3, distributed such that each box received 50 mL BD^- suspension of each relevant bacterium or bacteria at an effective optical density of 0.02 at 600 nm. Control plants boxes were uninoculated negative BD- control or uninoculated plants in nitrogen-rich medium (BDN). Only plant boxes containing two healthy seedlings were used for the plant infectivity experiments. Boxes were classified based on plant size and distributed among the treatments in such a way that the co-inoculations and corresponding control treatments (including *Frankia* sp. strain QA3 alone) each received a similar set of three boxes. Due to limitations in the number of boxes with similar plant size distribution, the single inoculation treatments received sets with average initial plant heights similar to each other (4.9-5.7 cm) but slightly smaller than the co-inoculations (5.3-6.1 cm). Thus, the final plant heights of non-*Frankia* single inoculations are comparable to each other but not strictly comparable to the co-inoculations (though the initial differences were small compared to final differences).

The plants were incubated at 28°C with a 16 h light period for 51 days. Plants were monitored for nodule development, growth, and health. After 51 days, approximate shoots heights were measured for each plant without removal from the box. Chlorophyll content was measured for a single representative leaf from each plant by positioning the leaf (without removal) between the light source and detector on a digital chlorophyll meter (AtLeaf), which measures absorbance at 640 nm.

Auxin production

Production of indole-related compounds by nine nodule isolates was estimated using a colorimetric assay with Salkowski reagent (0.01 M $FeCl_3$ in 35% perchloric acid) modified from Gang et al. (2019). Standard curves were generated using commercial indole-3-acetic acid (IAA) dissolved in KOH

and phosphate buffer solution (GoldBio) and indole-3-butyric acid (IBA) dissolved in ethanol; both were diluted in water to concentrations ranging from 0 to 100 µg/mL for IAA and the molar equivalent for IBA. The standards were then combined with equal parts Salkowski reagent, incubated in the dark for 30 minutes, and transferred to a cuvette to generate absorbance spectra with specific measurements at 530 nm (the maximum for IAA) and 450 nm (the maximum for IBA) using a Nanodrop spectrophotometer (Thermo Fisher). Visually, IAA standards appeared pink and IBA standards appeared orange-yellow color, in agreement with Gilbert et al. (2018). Bacterial cultures were pelleted and adjusted to a final optical density of 0.6 in 80% strength Czapek (strains 9, 12, 17, 21, 61, 70, 76) or MPN 10:10:5 (strains 24 and 85J) containing L-tryptophan (0.2 mg/mL final concentration), root exudates of nitrogen-stressed plants in BD^- (20% by volume), both, or water control, with three replicate tubes per treatment. Strains 9, 12, 17, 21, 61, 70, and 76 were incubated approximately 80 hours but had supernatant removed for qualitative assessment of auxin production at 40-50 hours. Strains 85J and 24 were incubated approximately 100 hours. Cultures were pelleted, and equal parts supernatant and Salkowski reagent were combined and incubated 30 minutes in the dark before observing color development and absorbance at 530, 450 nm, and 600 nm, using uninoculated 80% strength bacterial media with Salkowski reagent as a blank. IAA and IBA standards (5 and 20 µg/mL IAA equivalent) were prepared in bacterial media to verify similarity with standard curve values.

Because IAA and IBA have overlapping spectra, standard curves were generated using absorbance of both compounds at both 530 and 450 nm (Fig. 2). The slopes were used to generate a system of equations such that the total absorbance of a sample at 530 nm would equal the absorbance from IAA plus the absorbance for IBA, and the same for absorbance at 450 nm (Fig. 3). The equations were transformed to calculate approximate concentrations of IAA and IBA for each sample in µg/mL for IAA and the molar equivalent for IBA; concentration estimates then were converted to µM. For samples that returned a negative value for IAA concentration (likely an artifact of the assumption that only IBA and IAA contribute to absorbance at 450 nm), IAA concentration estimates were changed to zero, and IBA concentrations were recalculated using only the slope of the IBA curve. Generally, this only occurred when the samples appeared yellow, matching the color of the IBA standard alone, indicating that either no IAA was produced, or levels were so low they could not be detected with this technique. Additionally, any samples that appeared to contain bacterial cells based on visual observation and absorbance at 600 nm were excluded from final averages.

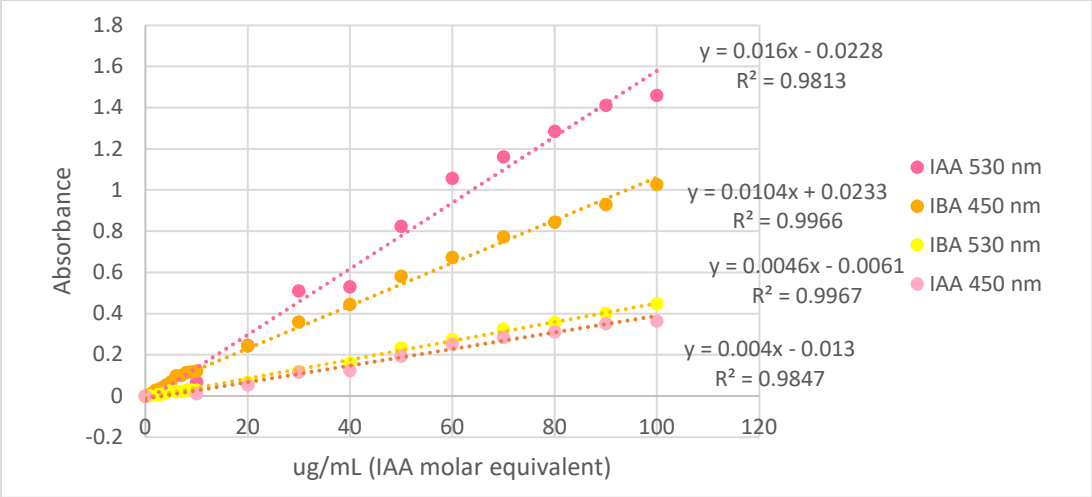

Fig. 2. Standard curves used to approximate concentrations of indole-3-acetic acid (IAA) and indole-3-butyric acid (IBA) produced by bacterial isolates based on absorbance of supernatants at 530 and

$$A_{530} = 0.16a + 0.0046b$$

$$A_{450} = 0.104b + 0.004a$$

$$b = (A_{450} - 0.25A_{530})/0.00925$$

$$a = (A_{530} - 0.0046b)/0.016$$

Fig. 3. Equations used to approximate concentrations of indole-3-acetic acid (IAA) and indole-3-butyric acid (IBA) produced by bacteria. a = IAA concentration (µg/mL), b = IBA concentration (molar equivalent of IAA µg/mL), A_{530} = absorbance at 530 nm, A_{450} = absorbance at 450 nm.

Siderophore production and phosphate solubilization

Blue CAS agar was prepared based on the protocol from Louden et al. 2011. The National Botanical Research Institute's phosphate growth medium (NBRIP) was prepared according to Nautiyal (1999) (glucose, 10 g: $Ca_3(PO_4)_2$, 5 g; $MgCl_2$ x $6H_2O$, 5 g; $MgSO_4$ x $7H_2O$, 0.25 g; KCl, 0.2 g $(NH_4)_2SO_4$, 0.1 g). Both medias were poured or pipetted into square 12 cm x 12 cm petri dishes while stirring. R2A, Czapek, and MPN 10:10:5 media were added to spaced apart wells in two 96-well plates, then inoculated with bacteria from the -80°C stocks using a sterile wooden stick. Liquid cultures of the slower-growing strains were added directly to wells and diluted to varying degrees with MPN media (10:10:5 for 85C, 85G, 85L, 85Q; 5 mM propionate for *Frankia* sp. strain QA3, and no dilution for *Frankia* sp. strain DC12). After overnight incubation, a pin replicator transferring 10 uL per well was used to prepare 1:30 dilutions in an additional well plate containing 0.02 M MOPS buffer adjusted to pH 6.8. Both the dilute and original plates were pin replicated onto CAS and NBRIP agar in duplicate, and onto MPN 10:10:5, Czapek, and R2A agar as controls. Strains that produced an orange halo on CAS agar were considered to produce siderophores, and strains that produced a clearing zone on NBRIP agar were considered to solubilize calcium phosphate. Halo sizes were qualitatively ranked as strong, moderate, or weak. Strains that grew on NBRIP but did not produce a halo were considered potential phosphate solubilizers based on the absence of other added phosphorus in the medium (other than agar), but this would need to be confirmed using a liquid assay.

Statistical analysis

Averages and standard deviations were calculated in Microsoft Excel. To correct for competition between plants, plant heights and percent increase in height were averaged for each box, and each box was considered a replicate. Nodulation timelines also used boxes as replicates due to the inability to distinguish between root systems mid-experiment. However, for chlorophyll measurements each plant was considered an individual replicate. Statistical analyses were performed in JMP using a threshold of $p < 0.05$. For plant experiments, separate one-way ANOVAs and corresponding Tukey tests were performed to compare final plant heights, chlorophyll content, and number of nodules at each observed time point. For the auxins assay, one-way ANOVAs and Tukey tests were used to compare the apparent concentrations of IAA and IBA between each treatment and the uninoculated negative controls. For each strain, student's paired t-tests were used to compare IAA and IBA production between the cultures supplemented with tryptophan only and cultures supplemented with tryptophan plus root exudates.

Genomic analysis

Of the nine bacterial strains used in the auxins assay, five have a published draft genome sequence -- 9, 12, 17, 21, and 24 (Davis et al. 2020). Enzymes associated with synthesis of indole-3-

acetic acid and phenyl acetic acid were identified in each genome using tblastn (BLAST: Basic Local Alignment Search Tool, Altschul et al. 1990) according to the accession numbers provided in the supplementary materials of Perrine-Walker et al. (2010, Table S1). (Enzymes associated with IBA production have not been specifically identified in bacteria.) The first, second, and third largest contigs were used to search for enzymes associated with PAA synthesis and the indole-pyruvic acid (IPA) pathway for IAA synthesis, but only the first and second contigs were used to search for enzymes in alternate IAA pathways, unless the strain lacked a complete IPA pathway. Only alignments with greater than 10% query cover and E-values less than or equal to 1e-5 were reported as hits. The largest contig of each genome assembly was also subjected to antiSMASH analysis to identify secondary metabolites (Blin et al. 2019, 2017, 2013; Weber 2015; Medema 2011).

Results

Bacterial Isolation

Bacterial strains isolated and stocked in this study (strains 51-110) are reported in Table 1. Based on sequencing of the 16S amplicon, newly identified strains belong to the genera *Kocuria* or *Rothia* (54), *Paenibacillus* (61), *Bacillus* (71, 76, 77), and *Staphylococcus* (52, 53), though many strains have yet to be identified.

Plant nodulation, growth, and health

Nodules began appearing on all *Frankia*-inoculated plants (including co-inoculations) between 7 and 11 days post inoculation (DPI) (Fig. 4). The largest increases in nodule count occurred within the first 26 days, after which the number of nodules increased more slowly and for some plants decreased slightly (Fig. 4). The maximum number of nodules per plant, 23.5, was observed in one replicate of the *Frankia* QA3 + 85J co-inoculation at 35 DPI, but by 50 DPI this had dropped to 19 nodules per plant, similar to the final maxima observed for the *Frankia* single inoculation (20.5) and co-inoculations with *Thiopseudomonas* (19) and *Paenibacillus* (20). The QA3 + *Streptomyces* co-inoculation had a lower final maximum nodule count (14.5) and produced fewer nodules overall, though the difference was not significant. No significant differences in nodule counts were found between any of the treatments at any time point.

Interestingly, nodule-like structures were observed on plants inoculated with strain 85J alone at 35 DPI, though they likely started forming some time before that (between 26 and 35 DPI) (Fig. 5). Unlike most of the nodules formed in the *Frankia*-inoculated plants, the pseudonodules produced by strain 85J were smaller and did not have emerging secondary roots. At 35 DPI, 21 pseudonodules per plant were present in one replicate box only, increasing to 26 by 50 DPI (data not shown). A few weeks later pseudonodules began appearing in an additional replicate box.

Negative control (BD^-) and *A. glutinosa* plants singly inoculated with non-*Frankia* bacteria grew only minimally over the course of the experiment (no more than 2 cm or 32% increase in height), while co-inoculated plants, the *Frankia* positive control, and the control in nitrogen-rich media increased in height between 56-83% on average, with the most robust plants more than doubling in size (Fig. 6B). In many of the boxes, especially those containing *Frankia*, one plant grew substantially more than the other, though the size discrepancy was somewhat less in the co-inoculation with *Thiopseudomonas* (21) and *Frankia* (data not shown). To correct for effects of competition in a small space, heights were averaged. Final average plant heights were significantly higher in the *Frankia*-inoculated plants than for plants without *Frankia*, but there were no significant height differences conferred by non-*Frankia* isolates in either the single or co-inoculations (Fig. 6A). Similarly, plant growth (% increase in height,

averaged in each box) was significantly higher in each *Frankia*-containing treatment compared to the corresponding single inoculations and negative control (Fig. 6B). However, co-inoculation with *Frankia* and each of the four non-*Frankia* isolates tested resulted in significantly higher chlorophyll content than the negative control, whereas the increase in chlorophyll content produced by *Frankia* alone was not significant (Fig. 6C).

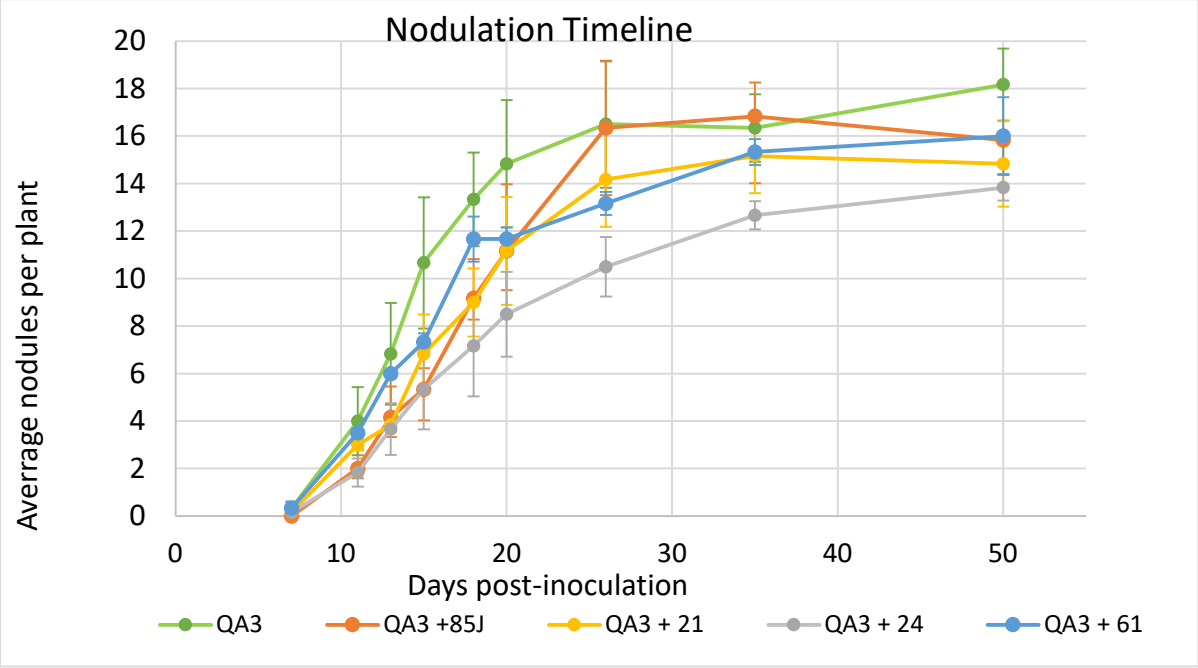

Fig. 4. Average number of nodules per plant at various time points after inoculation with bacteria. Only co-inoculations with *Frankia* (QA3) and an additional nodule isolate (85J, 21, 24, or 61) are shown. Error bars represent standard error.

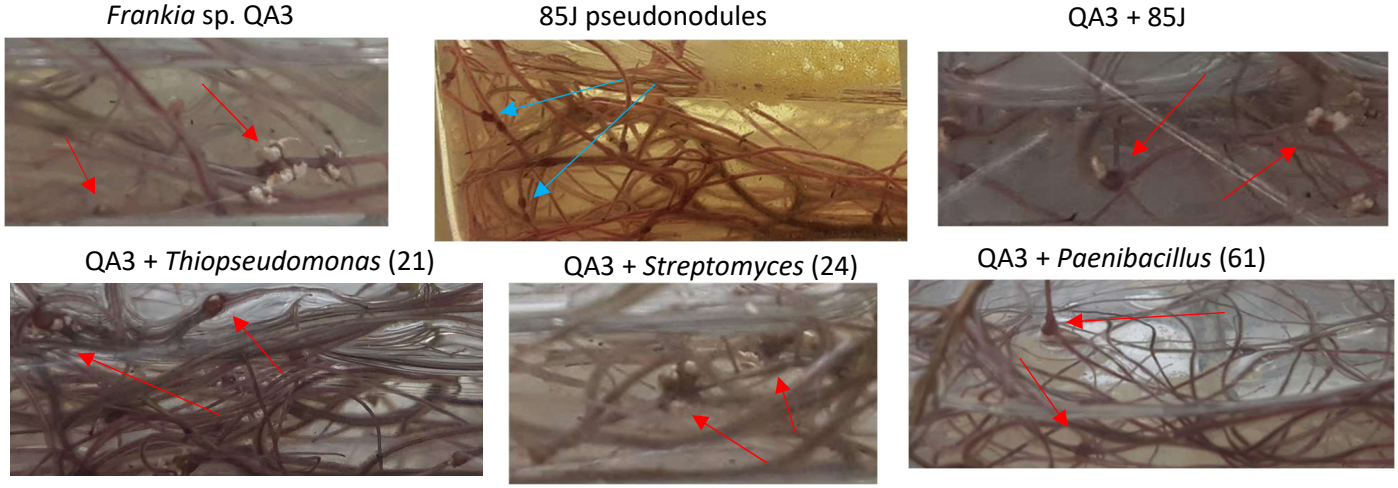

Fig. 5. Root nodules produced by *Frankia* QA3 alone or in co-inoculation with strains 21, 24, 61 or 85J on roots of *A. glutinosa* (red arrows); pseudonodules (top middle, blue arrows) produced by strain 85J alone on *A. glutinosa*.

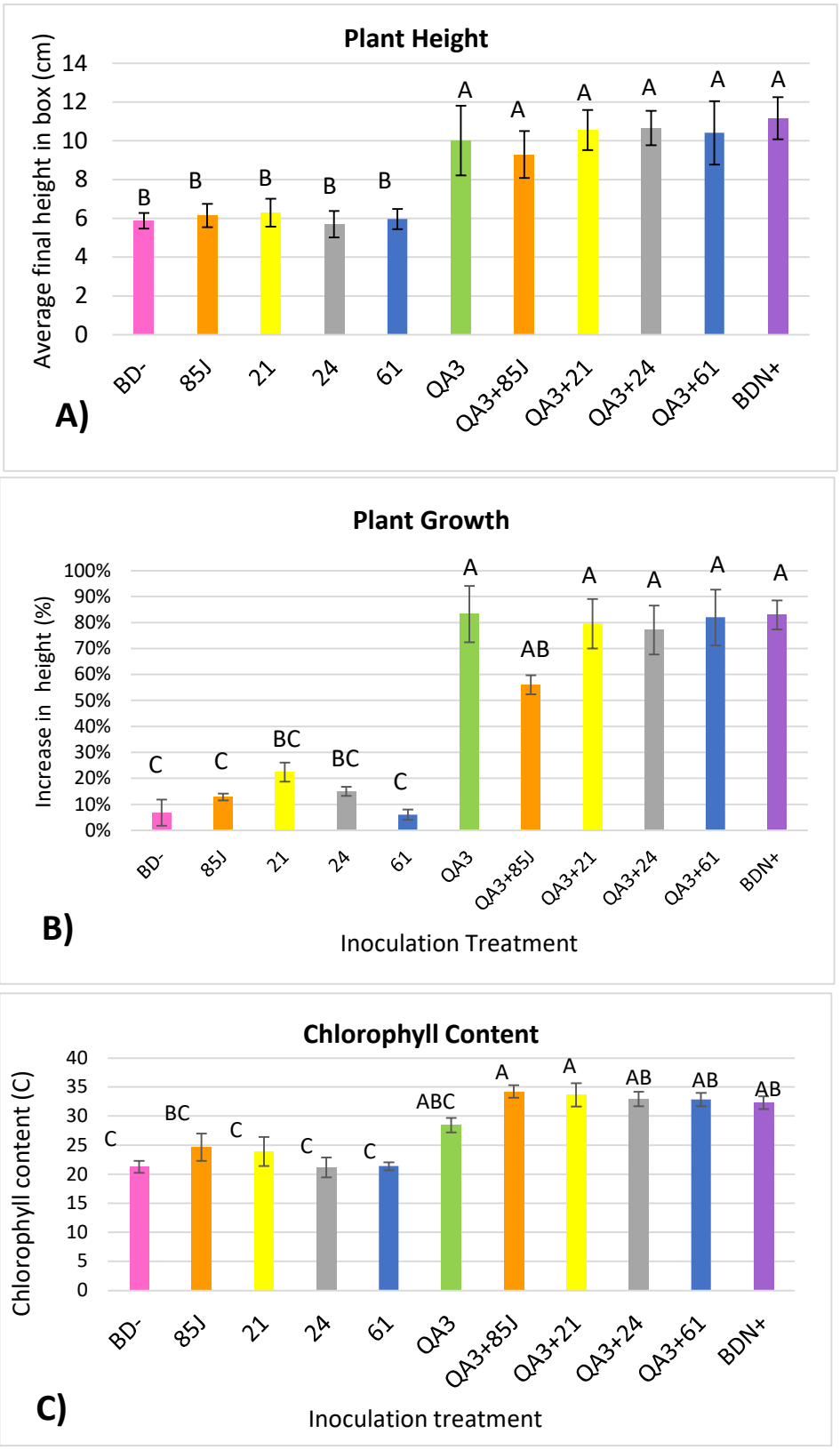

Fig. 6. A) Average plant height in box, B) average plant growth in box, and C) relative chlorophyll content of leaves (bottom) 51 days after inoculation with bacteria. BD- and BDN+ represent uninoculated controls without and with nitrogen, respectively. Values that do not share the same letters are statistically different (1-way ANOVA, $p < 0.05$). Error bars show standard error.

Auxin production

When supplemented with tryptophan (and sometimes without), *Herbaspirillum* (strain 12) and *Paenibacillus* (61) were significant producers of IBA, while *Kocuria* (17) and *Streptomyces* (24) were significant producers of IAA (or the related compounds indole-3-pyruvic acid or indole-3-acetamide, which also have a maximum absorbance at 530 nm) (Fig. 7). Strain 85J appeared to produce low levels of IAA, but the absorbance at 530 nm was not significant compared to the negative control. *Rhodococcus* (9), *Thiopseudomonas* (21), *Bacillus* (76), and strain 70 produced both IBA and IAA. IBA concentrations, which ranged approximately 45-200 µM for significant producers, were generally higher than IAA concentrations, which ranged approximately 3-50 µM for significant producers. *Bacillus* (76) produced significantly less IBA when exposed to root exudates in the presence of tryptophan compared to tryptophan alone ($p = 0.0202$); this was coupled with a near significant increase in IAA production ($p = 0.1254$) and a distinctive color difference (pink-orange instead of yellow) in two of the three replicates.

The genomes of *Herbaspirillum* (12), *Kocuria* (17), *Streptomyces* (24), and *Frankia* (QA3) putatively contain all three enzymes needed for IAA production by the indole-3-pyruvic acid (IPA) pathway: tryptophan aminotransferase, indole-3-pyruvate decarboxylase, and indole-3-acetaldehyde dehydrogenase (Table 3). However, *Rhodococcus* (9) appears to be missing the second enzyme, indicating that the compound detected in the auxins assay may actually be indole-3-pyruvic acid, with a different concentration than that shown in Fig. 7 due to differences in molar extinction coefficients. The *Rhodococcus* genome also encodes an amine oxidase, which converts tryptamine to indole-3-acetaldehyde in an alternative pathway, but it lacks the tryptophan decarboxylase needed to produce tryptamine from tryptophan. *Herbaspirillum* (12) and *Frankia* (QA3) additionally encode indole-3-acetamide hydrolase, and *Frankia* encodes tryptophan decarboxylase and an aryl acetonitrilase. The largest three contigs of the *Thiopseudomonas* genome do not encode any of the known enzymes used in Trp-dependent IAA synthesis pathways.

Each strain examined encodes one or more enzymes associated with synthesis of phenyl acetic acid – phenyl aminotransferase, phenyl pyruvate decarboxylase, and phenylacetaldehyde dehydrogenase. *Herbaspirillum* (12), *Kocuria* (17) and *Frankia* (QA3) encode all three enzymes; *Rhodococcus* (9) encodes the first and last; *Streptomyces* (24) encodes the second and third; and *Thiopseudomonas* (21) encodes only the first enzyme (Table 3).

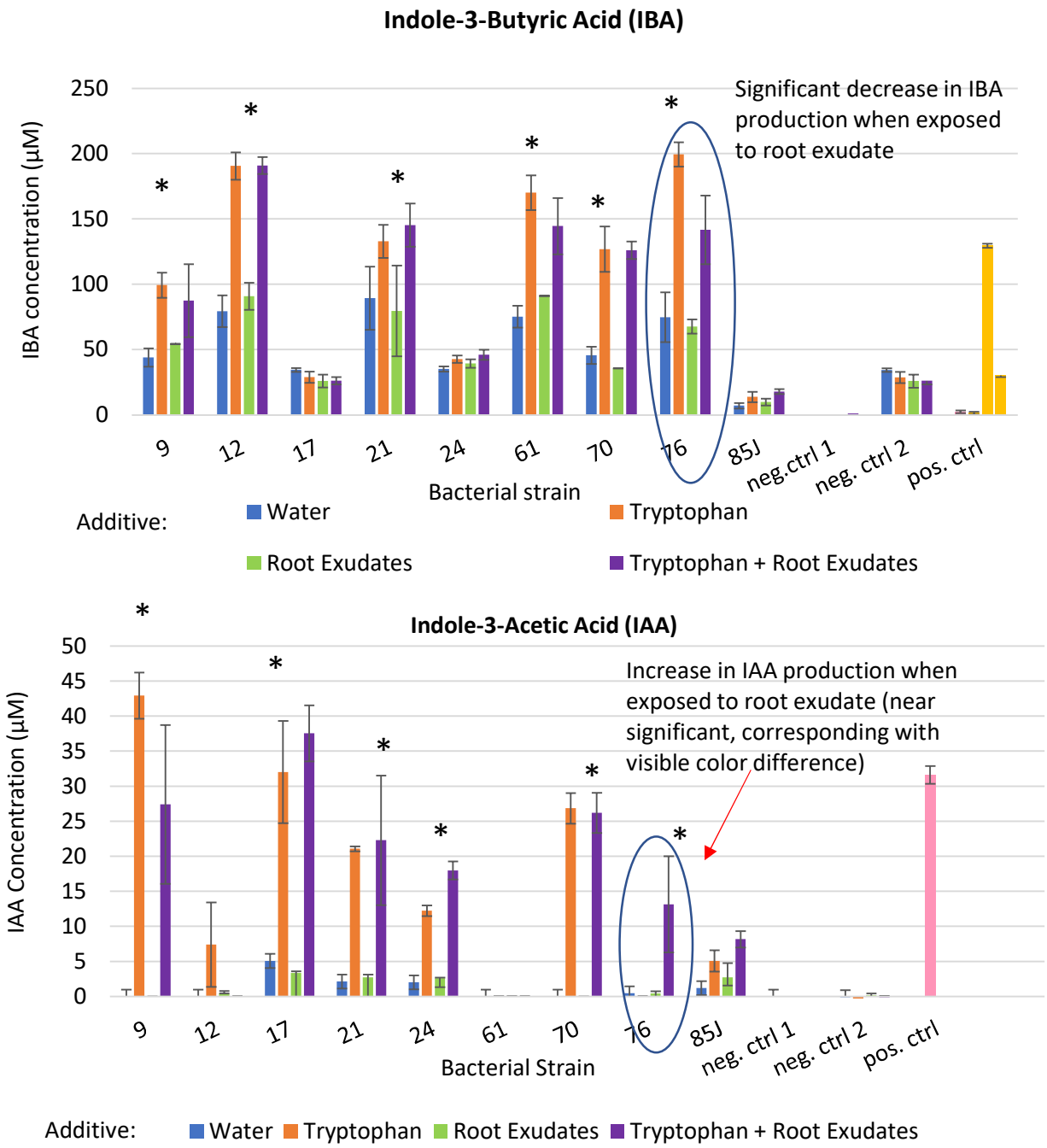

Fig. 7. Estimated concentrations of the plant hormones indole butyric acid (IBA) and indole-3-acetic acid (IAA) produced by nodule bacteria in growth medium supplemented with water control, tryptophan, root exudates of nitrogen-stressed *A. glutinosa* , or both tryptophan and root exudates. * indicates significant auxin production by the bacterial strain ($p < 0.05$). Circles indicate significant or near significant differences in auxin production of a single strain in response to root exudate exposure in the presence of tryptophan (student's paired t-test, $p < 0.05$).

Table 3. Enzymes associated with synthesis of the auxins indole-3-acetic acid (pink) and phenyl acetic acid (blue) located in genomes of select nodule isolates and the *Frankia* strain (QA3) used for plant inoculations. Enzymes associated with the IPA pathway for IAA synthesis are in light pink, and enzymes associated with other Trp-dependent pathways are in dark pink. Accession numbers from Perrine-Walker et al. 2010.

Strain	**9**	**12**	**17**	**21**	**24**	**QA3**
Enzyme Organism Accession number	Identity (%) Query cover (%) E-value					
Tryptophan aminotransferase *Azospirillum brasilense* AAW50704	28.12% 98% 3e-27	24.43% 91% 2e-30	25.21% 73% 2e-12	No hit	29.98% 97% 8e-49	30.79% 95% 8e-40
Indole-3-pyruvate decarboxylase *Enterobacter cloacae* P23234	No hit	23.22% 95% 1e-15	24.62% 87% 2e-7	No hit	22.97% 96% 4e-5	24.36% 96% 1e-19
Indole-3-acetaldehyde dehydrogenase *Ustilago maydis* AAC49575	39.10% 93% 5e-96	41.08% 99% 1e-104	37.92% 98% 6e-94	No hit	25.48% 75% 4e-12	44.58% 99% 8e-126
Indole-3-acetamide hydrolase *Agrobacterium tumefaciens* AAD30488	No hit	29.57% 90% 3e-28	No hit	No hit	No hit	26.57% 98% 1e-28
Tryptophan decarboxylase *Catharanthus roseus* AAA33109	No hit	No hit	No hit	No hit	No hit	22.05% 76% 1e-14
Amine oxidase *Klebsiella aerogenes* P49250	30.17% 83% 2e-79	No hit	No hit	No hit	No hit	No hit
Aryl acetonitrilase *Alicaligenes faecalis* BAA02684	No hit	No hit	No hit	No hit	No hit	29.55% 58% 1e-6
Phenyl aminotransferase *Lactococcus lactis* AAF06954	30.34% 92% 7e-45	29.33% 98% 3e-49	23.8% 52% 3e-5	33.71% 86% 4e-57	No hit	32.51% 96% 1e-51%
Phenyl pyruvate decarboxylase *Azospirillum brasilense* P51852	No hit	24.62% 87% 2e-7	23.73% 94% 1e-14	No hit	26.25% 84% 4e-7	28.16% 86% 5e-30
Phenylacetaldehyde dehydrogenase *Pseudomonas putida* ABR57228	35.00% 97% 2e-83	33.06% 96% 2e-74	24.73% 85% 7e-17	No hit	25.70% 53% 1e-5	35.23% 96% 4e-88

Siderophore production and phosphate solubilization

Four strains – 34, 69, 81, and 88A – were strong siderophore producers; strains 69 and 81 were also the strongest phosphate solubilizers, followed by strain 34 (Table 4, Fig. 8). On CAS medium, strain 34 initially produced a significant halo but later grew beyond its borders. Strains 88 and 98 produced more moderately-sized halos on CAS medium, and both *Herbaspirillum* strains (10, 12) and *Frankia* sp. DC12 (positive control) produced an orange zone underneath their spots but without a significant halo. No other strains grew on CAS medium. *Rhodococcus* (9), *Curtobacterium* (30), and strain 55 produced weak clearing zones on NBRIP. *Thioposeudomonas* (21), *Streptomyces* (23, 24), and strain 43 were tested but did not grow on the control media. All strains that grew on the control plates grew on NBRIP agar except 42, 107, and *Frankia* QA3.

Table 4. Siderophore production and phosphate solubilization by select strains.

Strain #	**Genus**	**Colony color**	**Siderophore production**	**Phosphate solubilization**	
				Growth	Halo
9	*Rhodococcus*	orange	No	Yes	Weak
10	*Herbaspirillum*	clear	Weak	Yes	No
12	*Herbaspirillum*	clear	Weak	Yes	No
17	*Kocuria*	yellow	No	Yes	No
30	*Curtobacterium*	yellow	No	Yes	Weak
34	unknown	white	Strong	Yes	Moderate
42	unknown	beige	No	No	No
54	*Kocuria* or *Rothia*	yellow	No	Yes	No
55	unknown	yellow	No	Yes	Weak
61	Paenibacillus	clear	No	Yes	No
69	unknown	translucent yellow	Strong	Yes	Strong
70	unknown	dark pink	No	Yes	No
71	*Bacillus*	light beige	No	Yes	No
81	unknown	cream	Strong	Yes	Strong
85J	unknown	orange/ salmon	No	Yes	No
88	unknown	cream	Moderate	Yes	No
88A	unknown	beige	Strong	Yes	No
98	unknown	cream	Moderate	Yes	No
107	unknown	red	No	No	No

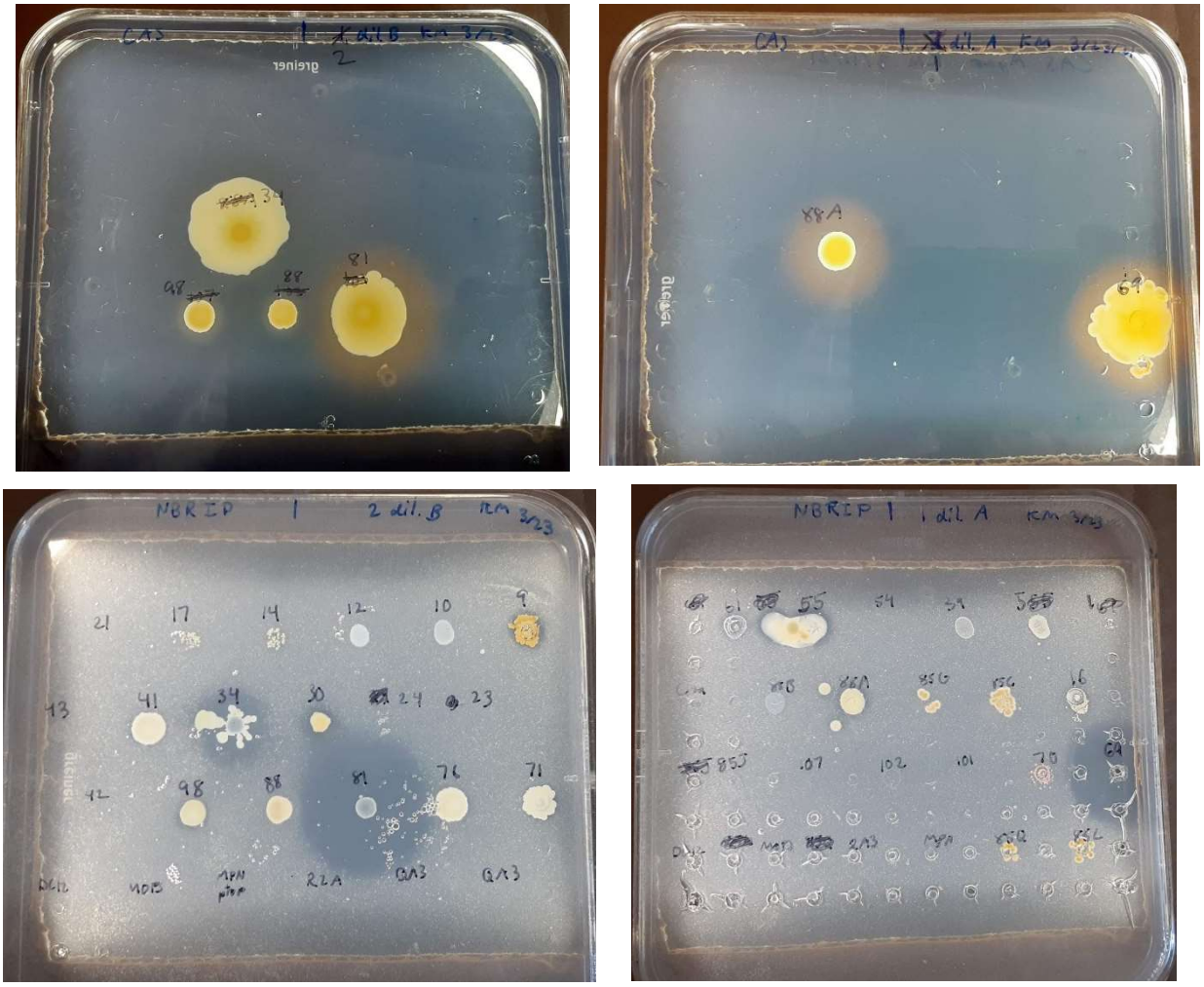

Fig. 8. Siderophore production (top) and phosphate solubilization assays (bottom), with positive results given by production of orange halo on CAS agar or clearing zone on NBRIP agar, respectively. Strain 34 (top left) initially produced a halo on CAS but grew past it before the photo was taken.

Prediction of secondary metabolites via antiSMASH

antiSMASH analysis revealed the presence of genes putatively encoding polyketide synthases (PKS) in the genomes of *Herbaspirillum* strain 12 (type I) and *Streptomyces* 24 (type III) (see appendix). *Streptomyces* (24) also encoded a heterocyst glycolipid synthase-like PKS (hglE-KS) and two genes with similarity to those used in synthesis of the antibacterial/antitumor agent lankacidin C (pyrroloquinoline quinone biosynthesis proteins B & E). *Rhodococcus* (9) and *Herbaspirillum* (12) genomes encoded non-ribosomal peptide synthetase clusters. The longest contigs of the *Kocuria* (17) and *Thiopseudomonas* (21) genomes did not contain any known secondary metabolite pathways.

Discussion:

In this study, we obtained 40 new bacterial isolates from alder nodules in fall 2019 to add to the collection started in spring 2018. Of the 28 new and existing isolates tested for siderophore production and calcium phosphate solubilization, three strains were capable of both, while five additional strains produced siderophores and three solubilized phosphate. We also found significant production of indole-

related compounds among eight out of nine isolates tested and located genes associated with auxin synthesis in the five of these isolates with sequenced genomes, though some genomes appeared to encode only incomplete pathways. The four isolates used to inoculate *A. glutinosa* plants increased leaf chlorophyll content in co-inoculation with *Frankia*, and one isolate, 85J, produced pseudonodules in the absence of *Frankia*.

The nearly universal production of indole-related compounds by the non-*Frankia* nodule isolates tested suggests that production of auxins or auxin precursors may in most cases be a prerequisite for successful nodule colonization. In *Casuarina glauca* nodules, phenyl acetic acid (PAA) and indole-3-acetic acid (IAA) accumulate in *Frankia*-infected plant cells due to production by *Frankia* and selective transport by plant cells (Perrine-Walker et al. 2010; Péret et al. 2007, 2008). Auxin production by non-*Frankia* colonizers could modulate this process by creating new zones of auxin accumulation in non-infected cells, supplementing *Frankia* auxin production within *Frankia*-infected cells, or adjusting the relative ratios of each auxin to regulate the timing of development events, such as the formation of secondary roots. Bacteria that do not possess a complete pathway, such as *Rhodococcus* (9) for IAA and strains 9, 21, and 24 for PAA, could theoretically be complemented by *Frankia*, other bacteria, or the plant host via cross-feeding, though it's important to recognize that enzymes could have been missed in the search parameters used for this study, and alternative pathways could exist that are not yet characterized. Auxins, and in particular IAA, have also been implicated as negative feedback regulators of nodulation by stimulating the degradation of the transcriptional repressor CgIAA7, allowing transcription of a yet-unidentified inhibitory signal (Champion et al. 2015). This hypothesis might explain the somewhat decreased nodulation observed in the *Steptomyces* (24) *Frankia* (QA3) co-inoculation.

In vitro, nodule isolates capable of IBA production generally produced much larger amounts of IBA than the corresponding amounts of IAA in the same or other strains. This is surprising given that IAA and PAA appear to play more important roles in nodule development than IBA (Perrine-Walker et al. 2010). However, IBA is often considered a storage form of IAA, and in plants it can be converted by removal of the two extra carbons using β -oxidation pathways similar to (or the same as) those used in fatty acid catabolism (Korasick et al. 2013). Although no specific enzymes for this conversion have yet been identified in bacteria, the ubiqity of β -oxidation suggests that bacteria could either perform this conversion themselves or produce IBA that the plant converts to IAA. *Bacillus* (76) decreased IBA production and appeared to switch on IAA production in response to root exudates from nitrogen-stressed *A. glutinosa* plants, which would be expected to contain the signals used in recruiting *Frankia*. Perhaps this strain produces IAA during the initial stages of nodule formation as a colonization technique, then switches to IBA production at some other point. In addition to its role as a storage form of IAA, IBA may or may not be bioactive in its own right, is transported separately from IAA, and is important in the formation of lateral and adventitious roots and establishment of the mycorrhizal symbiosis (Korasick et al. 2013, Ludwig-Müller 2000, Damodaran & Strader 2019). Since the nodule primordia depends on *Frankia* establishment in the pericycle, actinorhizal nodules are sites of lateral root formation (Franche & Bogusz 2011), and co-infection of *Frankia* with a strong IBA producer could enhance this process. For any nodule inhabitants that can also inhabit roots and/or rhizosphere, the resulting secondary roots would provide a fresh, ready-to-colonize habitat and an easy way to get there before other microorganisms take the space. Growth into roots after initial colonization of nodules has been observed for *Streptomyces* in pea plants (*Pisum sativum*) (Tokala et al. 2002, Tokala 2004).

Given the ability of strain 85J to produce pseudonodules, its apparent lack of auxin production is surprising. Small amounts of absorption at 530 nm were detected, and the fact that these were not

significantly different from one set of the auxins assay negative controls (MPN 10:10:5 medium plus additives) could be attributed to low-level contamination of the negative control combined with a slower growth and/or metabolic rate of 85J compared to the other isolates. (A separate set of negative controls had near-zero absorbance at both 530 nm and 450 nm, but only one replicate was tested, preventing use of this set in statistical tests.) Even if 85J does not produce IAA or IBA, it could produce PAA, which has not been shown to produce a colored complex with Salkowski reagent and accumulates more in nodules than IAA (Perrine-Walker et al. 2010). However, pseudonodule-producing strains may use different strategies for infection than other non-*Frankia* nodule isolates. Of the two *Norcardia* strains shown to produce pseudonodules on *C. glauca*, strain BMG51109 produced IAA, PAA, and comparatively low levels of IBA, while BMG111209 strain only produced IBA at even lower levels (Ghodhbane-Gtari et al. 2019). Strikingly, the strain producing very little auxin, BMG111209, induced expression of the CgNIN promoter (associated with response to *Frankia* signals) in infected root cells, while the higher auxin producer BMG51109 did not (Ghodhbane-Gtari et al. 2019). Like the pseudonodules induced by *Norcardia* on *C. glauca*, pseudonodules produced by 85J on *A. glutinosa* lacked a multilobe structure, and the lack of emerging secondary roots in 85J pseudonodules is consistent with the observation that *Norcardia* infected primarily root cortical cells without reaching the pericycle (Ghodhbane-Gtari et al. 2019).

The increased chlorophyll content in plants coinoculated with *Frankia* QA3 and strain 85J, *Thiopseudomonas* (21), *Streptomyces* (24), or *Paenibacillus* could be attributed to increased nitrogen fixation, as leaf chlorosis is a common symptom of nitrogen deficiency. The control plants in nitrogen-rich media had similarly high chlorophyll content, while control plants in nitrogen-poor media had low chlorophyll content. Given that the total number of nodules was not significantly affected by co-inoculation with non-*Frankia* strains, increased N fixation could be achieved via improved *Frankia* nodule occupancy, larger nodule size, and/or increased nitrogenase activity. Siderophore production and phosphate solubilization would be expected to improve nitrogenase activity by supplying essential cofactors and ensuring adequate ATP supply (Sun et al. 1992, Tokala et al. 2002, Tokala 2004, Djurdjevic et al. 2020), but these traits were not observed in *Paenibacillus* (61) or strain 85J, and *Streptomyces* (24) and *Thiopseudomonas* (21) need to be retested. Phosphate solubilization may also be less important in the hydroponic system used for this study because BD^- medium contains ample soluble phosphate. antiSMASH analysis revealed putative polyketide synthases (PKS) in the *Streptomyces* (24, type III) genome as well as the genome of the siderophore-producing *Herbaspirillum* (12, type I); polyketide synthases are associated with production of siderophores, antibiotics, and a number of other secondary metabolites (Nivina et al. 2019, Mahmoud et al. 2015). Although *Frankia* QA3 is known to produce its own siderophores, the *Frankia* strain in the alders used for isolation has not yet been identified, though capacity for siderophore production is likely given that many *Frankia* strains utilize an unusually large number of metalloproteins in addition to nitrogenase (Furnholm & Tisa 2014). In either case, siderophore production by non-*Frankia* isolates could allow *Frankia* to devote more energy to nitrogen fixation. The *Streptomyces* (24) genome additionally contained a PKS resembling heterocyst glycolipid synthase, which is used by cyanobacteria in the compartmentalization of nitrogen fixation away from oxygenic metabolism (Campbell et al. 1997). It is tempting to speculate that glycolipids produced by *Streptomyces* could supplement hopanoids produced by *Frankia* for vesicle formation and protection of nitrogenase (Berry et al. 1993), and this could be an interesting area for further study.

Overall, diverse nodule endophytes appear to play important roles in *Alnus* nodule formation and function. Although much remains speculative at this point, obtaining physiological information for a

select set of strains isolated from the same source can provide valuable insight to complement non-culture approaches of community profiling, such as 16S amplicon sequencing or metagenomics. Future work could include measurements of nitrogen fixation in co-inoculated plants via the acetylene reduction assay and examining seasonal changes in the nodule and root microbial communities. Understanding how nodules function as a community rather than simply a two-way interaction can help us optimize nitrogen fixation and inform our use of actinorhizal and legume plants in agriculture and bioremediation.

Acknowledgements:

This project is supported by the USDA NIFA Hatch NH686 project.

Special thanks to

- Dr. Tisa, as well as present and past members of Tisa Lab who have helped in various ways: Celine, Ian, Eric, Megan, Lilly, Ryan, Sophia, Ethan, Victoria, Jessica, & Delaney
- Drs. Nathalie Diagne and Mariama Ngom for showing me exciting applications of actinorhizal plants & their microbes
- All my professors who have piqued my curiosity in plant-microbe interactions and microbial communities, especially Drs. Anissa Poleatewich, Jessica Ernakovich, Becky Sideman, Cheryl Smith, Cheryl Whistler, Richard Smith, & Feixia Chu
- My family and friends for supporting me along the way

References:

Ahmadi, M.K., Fawaz, S., Jones, C.H., Zhang, G. & Pfeifer, B.A. (2015). Total Biosynthesis and Diverse Applications of the Nonribosomal Peptide-Polyketide Siderophore Yersiniabactin. Applied and Environmental Microbiology, 81 (16) 5290-5298; DOI: 10.1128/AEM.01373-15

Altschul, S.F., Gish, W., Miller, W., Myers, E.W. & Lipman, D.J. (1990) "Basic local alignment search tool." J. Mol. Biol. 215:403-410.

Berry, A. M., Harriott, O. T., Moreau, R. A., Osman, S. F., Benson, D. R., & Jones, A. D. (1993). Hopanoid lipids compose the Frankia vesicle envelope, presumptive barrier of oxygen diffusion to nitrogenase. Proceedings of the National Academy of Sciences of the United States of America, 90(13), 6091–6094. https://doi.org/10.1073/pnas.90.13.6091

Bhadha, J. H., Capasso, J. M., Khatiwada, R., Swanson, S., & LaBorde, C. (2017). Raising soil organic matter content to improve water holding capacity. *UF/IFAS*, 1-5.

Blin, K., Medema, M. H., Kazempour, D., Fischbach, M. A., Breitling, R., Takano, E., & Weber, T. (2013). antiSMASH 2.0—a versatile platform for genome mining of secondary metabolite producers. *Nucleic acids research*, *41*(W1), W204-W212.

Blin, K., Shaw, S., Steinke, K., Villebro, R., Ziemert, N., Lee, S. Y., ... & Weber, T. (2019). antiSMASH 5.0: updates to the secondary metabolite genome mining pipeline. *Nucleic acids research*, *47*(W1), W81-W87.

Blin, K., Wolf, T., Chevrette, M. G., Lu, X., Schwalen, C. J., Kautsar, S. A., ... & Medema, M. H. (2017). antiSMASH 4.0—improvements in chemistry prediction and gene cluster boundary identification. *Nucleic acids research*, *45*(W1), W36-W41.

Bourke, R.M. 1985. Food, coffee and casuarina: an agroforestry system from the Papua New Guinea highlands. Agroforestry Systems **2**: 273-279. https://link.springer.com/content/pdf/10.1007%2FBF00147038.pdf

Campbell, E., Cohen, M.F., & Meeks, J.C. (1997). A polyketide-synthase-like gene is involved in the synthesis of heterocyst glycolipids in Nostoc punctiforme strain ATCC 29133. Archives of Microbiology 167(4):251-8. DOI: 10.1007/s002030050440

Castellano-Hinojosa, A., & Strauss, S. L. (2020). Impact of cover crops on the soil microbiome of tree crops. *Microorganisms*, *8*(3), 328.

Champion, A., Lucas, M., Tromas, A., Vaissayre, V., Crabos, A., Diédhiou, I., ... & Laplaze, L. (2015). Inhibition of auxin signaling in Frankia species-infected cells in Casuarina glauca nodules leads to increased nodulation. *Plant physiology*, *167*(3), 1149-1157.

Cissoko, M., Hocher, V., Gherbi, H., Gully, D., Carré-Mlouka, A., Sane, S., ... & Svistoonoff, S. (2018). Actinorhizal signaling molecules: *Frankia* root hair deforming factor shares properties with NIN inducing factor. Frontiers in plant science, 9, 1494.

D'Angelo T., F. Ghodhbane-Gtari, A. Ktari, K. Hezbri, A. Gueddou, M. Gtari, and L.S. Tisa. (2016). Metagenomic Analysis of the Root Nodule Endophyte Community of the Actinorhizal plant Casuarina glauca. The 116th General Meeting of the American Society for Microbiology June 16-20, 2016 in Boston, MA.

Damodaran, S., & Strader, L. C. (2019). Indole 3-butyric acid metabolism and transport in Arabidopsis thaliana. Frontiers in plant science, 10, 851.

Diagne, N., Diouf, D., Svistoonoff, S., Kane, A., Noba, K., Franche, C., ... & Duponnois, R. (2013). Casuarina in Africa: distribution, role and importance of arbuscular mycorrhizal, ectomycorrhizal fungi and Frankia on plant development. *Journal of environmental management*, *128*, 204-209.

Diagne, N., Ngom, M., Djighaly, P. I., Ngom, D., Ndour, B., Cissokho, M., ... & Champion, A. (2015). Remediation of heavy metal-contaminated soils and enhancement of their fertility with actinorhizal plants. In *Heavy Metal Contamination of Soils* (pp. 355-366). Springer, Cham.

Djurdjevic, I., Trncik, C., Rohde, M., Gies, J., Grunau, K., Schneider, F., ... & Einsle, O. (2020). The Cofactors of Nitrogenases. *Transition Metals and Sulfur–A Strong Relationship for Life*, *20*, 257.

Franche, C., & Bogusz, D. (2012). Signalling and communication in the actinorhizal symbiosis. In Signaling and communication in plant symbiosis (pp. 73-92). Springer, Berlin, Heidelberg.

Furnholm, T. R., & Tisa, L. S. (2014). The ins and outs of metal homeostasis by the root nodule actinobacterium Frankia. BMC genomics, 15, 1092. https://doi.org/10.1186/1471-2164-15-1092

Gagnon, V., Rodrigue-Morin, M., Tremblay, J., Wasserscheid, J., Champagne, J., Bellenger, J. P., ... & Roy, S. (2020). Vegetation drives the structure of active microbial communities on an acidogenic mine tailings deposit. PeerJ, 8, e10109.

Ghodhbane-Gtari, F., Nouioui, I., Hezbri, K., Lundstedt, E., D'angelo, T., McNutt, Z., ... & Tisa, L. S. (2019). The plant-growth-promoting actinobacteria of the genus Nocardia induces root nodule formation in Casuarina glauca. Antonie Van Leeuwenhoek, 112(1), 75-90

Gilbert, S., Xu, J., Acosta, K., Poulev, A., Lebeis, S., & Lam, E. (2018). Bacterial Production of Indole Related Compounds Reveals Their Role in Association Between Duckweeds and Endophytes. Frontiers in chemistry, 6, 265. https://doi.org/10.3389/fchem.2018.00265

Glickmann, E., & Dessaux, Y. (1995). A critical examination of the specificity of the salkowski reagent for indolic compounds produced by phytopathogenic bacteria. Applied and environmental microbiology, 61(2), 793-796.

Glickmann, E., & Dessaux, Y. (1995). A critical examination of the specificity of the salkowski reagent for indolic compounds produced by phytopathogenic bacteria. Applied and environmental microbiology, 61(2), 793-796.

Goswami, D., Thakker, J. N., & Dhandhukia, P. C. (2015). Simultaneous detection and quantification of indole-3-acetic acid (IAA) and indole-3-butyric acid (IBA) produced by rhizobacteria from l-tryptophan (Trp) using HPTLC. Journal of microbiological methods, 110, 7-14.

Gregor, A. K., Klubek, B., & Varsa, E. C. (2003). Identification and use of actinomycetes for enhanced nodulation of soybean co-inoculated with *Bradyrhizobium japonicum*. *Canadian journal of microbiology*, *49*(8), 483-491.

Ingleby, K., Wilson, J., Munro, R. C., & Cavers, S. (2007). Mycorrhizas in agroforestry: spread and sharing of arbuscular mycorrhizal fungi between trees and crops: complementary use of molecular and microscopic approaches. *Plant and soil*, *294*(1), 125-136.

Janati, W., Benmrid, B., Elhaissoufi, W., Zeroual, Y., Nasielski, J., & Bargaz, A. 2021. Will Phosphate Bio-Solubilization Stimulate Biological Nitrogen Fixation in Grain Legumes? Front. Agron. 3, 637196. doi: 10.3389/fagro.2021.637196

Knowlton, S., & Dawson, J. O. (1983). Effects of Pseudomonas cepacia and cultural factors on the nodulation of Alnus rubra roots by Frankia. *Canadian Journal of Botany*, *61*(11), 2877-2882.

Knowlton, S., Berry, A., & Torrey, J. G. (1980). Evidence that associated soil bacteria may influence root hair infection of actinorhizal plants by Frankia. *Canadian journal of microbiology*, *26*(8), 971-977.

Korasick, D. A., Enders, T. A., & Strader, L. C. (2013). Auxin biosynthesis and storage forms. Journal of experimental botany, 64(9), 2541-2555.

Kumar, A., Patel, J. S., & Meena, V. S. (2018). Rhizospheric microbes for sustainable agriculture: an overview. *Role of rhizospheric microbes in soil*, 1-31.

Louden, B. C., Haarmann, D., & Lynne, A. M. (2011). Use of blue agar CAS assay for siderophore detection. Journal of microbiology & biology education: JMBE, 12(1), 51.

Ludwig-Müller, J. (2000). Indole-3-butyric acid in plant growth and development. Plant Growth Regulation, 32(2), 219-230.

Medema, M. H., Blin, K., Cimermancic, P., de Jager, V., Zakrzewski, P., Fischbach, M. A., ... & Breitling, R. (2011). antiSMASH: rapid identification, annotation and analysis of secondary metabolite biosynthesis gene clusters in bacterial and fungal genome sequences. *Nucleic acids research*, *39*(suppl_2), W339-W346.

Murray, M. G., & Thompson, W. F. (1980). Rapid isolation of high molecular weight plant DNA. *Nucleic acids research*, *8*(19), 4321-4326.

Nautiyal, C. S. (1999). An efficient microbiological growth medium for screening phosphate solubilizing microorganisms. FEMS microbiology Letters, 170(1), 265-270.

Ngom, M., Gray, K., Diagne, N., Oshone, R., Fardoux, J., Gherbi, H., ... & Champion, A. (2016). Symbiotic performance of diverse Frankia strains on salt-stressed Casuarina glauca and Casuarina equisetifolia plants. *Frontiers in plant science*, *7*, 1331.

Nivina, A., Yuet, K.P., Hsu, J. and Khosla, C. (2019). Evolution and Diversity of Assembly-Line Polyketide Synthases. Chem. Rev. 119, 24, 12524–12547. https://doi.org/10.1021/acs.chemrev.9b00525

Péret, B., Svistoonoff, S., Lahouze, B., Auguy, F., Santi, C., Doumas, P., & Laplaze, L. (2008). A Role for auxin during actinorhizal symbioses formation?. Plant signaling & behavior, 3(1), 34-35.

Péret, B., Swarup, R., Jansen, L., Devos, G., Auguy, F., Collin, M., ... & Laplaze, L. (2007). Auxin influx activity is associated with Frankia infection during actinorhizal nodule formation in Casuarina glauca. *Plant physiology*, *144*(4), 1852-1862. doi:10.1104/pp.107.101337

Perrine-Walker F, Doumas P, Lucas M, et al. (2010) Auxin carriers localization drives auxin accumulation in plant cells infected by Frankia in Casuarina glauca actinorhizal nodules. Plant Physiol. 2010;154(3):1372-1380. doi:10.1104/pp.110.163394

Saravanan, S. and A. Vijayaraghavan. (2014). Casuarina equisetifolia-based agroforestry systems for higher economic returns for the farming communities in Tamilnadu, India. Fifth International Casuarina Workshop, Mamamallapuram, Chennai, India. http://envis.nic.in/ifgtb/pdfs/Casuarina%20equisetifolia-based%20agroforestry%20systems%20for%20higher%20economic%20returns%20for%20the%20farming%20communities%20in%20Tamilnadu,%20India.pdf

Sen, A., Beauchemin, N., Bruce, D., Chain, P., Chen, A., Davenport, K. W., ... & Tisa, L. S. (2013). Draft genome sequence of *Frankia* sp. strain QA3, a nitrogen-fixing actinobacterium isolated from the root nodule of *Alnus nitida*. Genome announcements, 1(2).

Soe, K. M., & Yamakawa, T. (2013). Evaluation of effective Myanmar Bradyrhizobium strains isolated from Myanmar soybean and effects of coinoculation with Streptomyces griseoflavus P4 for nitrogen fixation. *Soil science and plant nutrition*, *59*(3), 361-370.

Soe, K. M., Bhromsiri, A., Karladee, D., & Yamakawa, T. (2012). Effects of endophytic actinomycetes and Bradyrhizobium japonicum strains on growth, nodulation, nitrogen fixation and seed weight of different soybean varieties. *Soil Science and Plant Nutrition*, *58*(3), 319-325.

Sun, J.S., Simpson, R.J. & Sands, R. (1992). Nitrogenase activity of two genotypes of *Acacia mangium* as affected by phosphorus nutrition. Plant Soil 144, 51–58 https://doi.org/10.1007/BF00018844

Tokala, R. K. (2004). *Enhancement of nitrogen fixation in legumes and production of antifungal compounds by rhizosphere-colonizing actinomycetes* (Doctoral dissertation, University of Idaho, 3123854).

Tokala, R. K., Strap, J. L., Jung, C. M., Crawford, D. L., Salove, M. H., Deobald, L. A., Bailey, J.F. & Morra, M. J. (2002). Novel plant-microbe rhizosphere interaction involving *Streptomyces lydicus* WYEC108 and the pea plant (Pisum sativum). *Applied and environmental microbiology*, *68*(5), 2161.doi: 10.1128/AEM.68.5.2161-2171.2002

Valdés, M., Pérez, N. O., Estrada-de Los Santos, P., Caballero-Mellado, J., Pena-Cabriales, J. J., Normand, P., & Hirsch, A. M. (2005). Non-Frankia actinomycetes isolated from surface-sterilized roots of Casuarina equisetifolia fix nitrogen. Applied and environmental microbiology, 71(1), 460-466.

Valdés, M., Pérez, N. O., Estrada-de Los Santos, P., Caballero-Mellado, J., Pena-Cabriales, J. J., Normand, P., & Hirsch, A. M. (2005). Non-Frankia actinomycetes isolated from surface-sterilized roots of Casuarina equisetifolia fix nitrogen. Applied and environmental microbiology, 71(1), 460-466.

Weber, T., Blin, K., Duddela, S., Krug, D., Kim, H. U., Bruccoleri, R., ... & Medema, M. H. (2015). antiSMASH 3.0—a comprehensive resource for the genome mining of biosynthetic gene clusters. *Nucleic acids research*, *43*(W1), W237-W243.

Appendix:

Media recipes:

MPN bacterial medium (MOPS + Phosphate + Nitrogen)

14.7g MOPS buffer (MW 209.3) OR 16.1g MOP sodium salt (MW 231.25)
5.95g K_2HPO_4
0.94g NH_4Cl
Bring to 3.5L
pH to 7 with NaOH

In a 500ml flask, add 100ml MPN
Autoclaved flasks

Add Carbon source
Propionate final concentration: 5mM
Other C- sources final concentration: 20mM or 10 mM

Add 1.7mL of Metal mix stock solution to 100ml MPN

All C-sources stock solution are prepared at 0.5M
Metal mix stock solution

- 20ml 0.1M Na_2MoO_4
- 8ml 0.5M $MgSo_4$
- 4ml 20mM $FeCl_3$-NTA
- 2ml 10x MOB-MBA

- 20mM $FeCl_3$-NTA

1. Make 50mM solution of NTA (Nitrilotriacetic acid) using 1.91g per 200ml
2. Adjust to pH 6.5
3. Add 10mM $FeCl_3$
4. Mix with metal bar
5. Autoclaved

- 10X MOB-MBA

1. $Fe_2(So_4)_3$ → 2.5g
2. $MnCl_2$, $4H_2O$ → 5.0g
3. $CuCl_2$, $2H_2O$ → 250mg
4. $CaCl_2$, $2\ H_2O$ → 10g
5. H_3BO_3 → 500mg
6. $ZnSO_4$, $7\ H_2O$ → 1g
7. $CoCl_2$, $6H_2O$ → 200mg
8. Prepared in 0.1N HCl in 1000ml

CAS medium for siderophore detection
Adapted from Louden et al. (2011), who adapted it from the original Schwinn & Neilands paper

Clean all glassware and stir bars with 6M HCl to remove any trace elements, then rinse with MilliQ H2O. Plasticware does not need to be rinsed in HCl.

A. Blue Dye:
    a. Solution 1:
        i. Dissolve 0.06 g of CAS (Fluka Chemicals) in 50 mL MilliQ H_2O.
    b. Solution 2:

i. Dissolve 0.27 g of FeCl3-6 H_2O in 100 mL MilliQ H_2O. Filter sterilize.
Combine 98.5 µL 37% HCl with 89 mL + 901.5 µL MilliQ H_2O.
Combine 9 mL HCl solution and 1 mL $FeCl_3$ for a final concentration of 0.0027 g $FeCl_3$ in 10 mM HCl.

c. Solution 3:

i. Dissolve 0.73 g of HDTMA in 400 mL MilliQ H_2O.

d. Mix Solution 1 with 9 ml of Solution 2. Then mix with 40 mL Solution 3. Solution should now be blue to blue-violet. Autoclave and store in a plastic container/bottle.

B. Mixture solution:

a. Minimal Media 9 (MM9) Salt Solution Stock

i. Dissolve 12 g KH_2PO_4, 20 g NaCl, and 40 g NH_4Cl in 400 ml of MilliQ H_2O. Autoclave.

b. 20% Glucose Stock

i. Dissolve 20 g glucose in 100 ml of ddH2O. Autoclave.

c. NaOH Stock

i. Dissolve 25 g of NaOH in 150 ml ddH2O; pH should be ~12.

d. Casamino Acid Solution

i. Dissolve 9 g of Casamino acid in 81 ml of ddH2O.
ii. Extract with 3% 8-hydroxyquinoline in chloroform to remove any trace iron.
iii. Filter sterilize.

C. CAS agar Preparation:

a. Add 40 mL of MM9 salt solution to 300 mL MilliQ H_2O in acid-rinsed 500 mL bottle.

b. Dissolve 12.90 g piperazine-N,N'-bis(2-ethanesulfonic acid) PIPES.

i. PIPES will not dissolve below pH of 5. Using the NaOH and HCl stocks prepared in acid-rinsed bottles, bring pH up to 6 and slowly add PIPES while stirring. The pH will drop as PIPES dissolves. While stirring, slowly bring the pH up to 6.8. Do not exceed 6.8 as this will turn the solution green.

c. Add 6 g Bacto agar.

d. Autoclave and cool to 50°C while stirring.

e. Add 12 mL sterile Casamino acid solution and 4 mL sterile 20% glucose solution to MM9/ PIPES mixture.

f. Slowly add 40 ml of Blue Dye solution along the glass wall with enough agitation to mix thoroughly.

g. Aseptically pour plates. (50 mL/square plate).

BDN/BD$^-$ plant medium

BD(N) medium

1. 0.68g of MES per Liter
2. If making BDN$^+$, add 0.5g KNO_3 per liter
3. Add 995ml of Milli-Q water
4. pH to 6.6 to 6.8
5. autoclaved

---

6. Let media cold
7. Add 1ml of each stock solution per liter of media
   - $CaCl_2$, 2 H_2O
   - KH_2PO_4
   - $MgSO_4$, 7 H_2O
     K_2SO_4
     $MnSO_4$, H_2O
   - FeEDTA
   - Oligoelements mix

Stock solutions (preparation of 100ml of each except for the oligoelement mix : 500ml)

- $CaCl_2$, 2 H_2O → 147g/L
- KH_2PO_4 → 68g/L
- $MgSO_4$, 7 H_2O → 61.5g/L
  K_2SO_4 → 43.5g/L
  $MnSO_4$, H_2O → 0.17g/L
- FeEDTA
  Na_2EDTA → 9.31g/L
  $FeSO_4$ → 6.96g/L
- Oligoelements mix
  H_3BO_3 → 0.124g/L
  $ZnSO_4$, 5 H_2O → 0.144 g/L
  $CuSO_4$, 5 H_2O → 0.05 g/L
  $CoCl_2$ → 0.028 g/L
  Na_2MoO_4, 2 H_2O → 0.024 g/L

Plant inoculations with EuN1f and *Streptomyces* 24

An additional experiment aimed to explore the possibility that non-*Frankia* bacteria isolated from alder nodules might facilitate nodulation by an alternative *Frankia* strain isolated from a non-alder host. Such a relationship would support the hypothesis that non-*Frankia* bacteria play a direct role in the *Frankia* infection process. The *Frankia* genus includes four taxonomic clusters that differ in their host range, infectivity, and nitrogen fixing capacity. The primary *Alnus*-infective *Frankia* strains, including strain QA3, belong to cluster 1, which also include strains that infect plants from the Casuarinaceae and Myricaceae families (Mansour et al. 2020). Cluster 3 is considered the most "promiscuous" group and contains strains infective on Elaeagnaceae, Rhamnaceae, Myricaceae, Gynmnostoma, and occasionally the genus *Alnus* (Mansour et al. 2020). Cluster 3 *Frankia* strains E1, E2, E3, and E4 isolated from an *Eleagnus* hybrid in Italy formed small nodules on some *Alnus glutinosa* and *Alnus incana* plants, though the plants remained small and yellow, and an acetylene reduction assay revealed no nitrogen fixation (Bosco et al. 1992). Cluster 3 *Frankia* strains have also been detected in *Alnus incana* nodules from a polluted environment (Ridgway et al. 2004). *Frankia* sp. EuN1f, isolated from *Eleagnus umbellata* in Illinois, USA, belongs to cluster 3. In this study, EuN1f was tested for infectivity on *Alnus glutinosa* alone and in conjunction with *Streptomyces* sp. (strain 24) from nodules of *Alnus incana* in New Hampshire. We aimed to determine whether *Frankia* sp. EuN1f would form nodules on A. *glutinosa* and whether *Streptomyces* (24) would enhance nodulation.

To promote germination, *Alnus glutinosa* seeds (Sheffield, Hungary) were stored for several weeks at 4°C, then soaked for 24 hours in sterile deionized water. The seeds were sterilized by incubating in 15 mL 30% hydrogen peroxide with 2 drops Tween-20 for 30 minutes, then rinsed six times with sterile deionized water. The seeds were spread in sterile Magenta GA-7 boxes containing perlite wetted with Brougton and Dilworth with nitrogen (BDN) nutrient medium (Broughton & Dilworth 1971). After germination and appearance of the first true leaves (approximately 4 weeks), seedlings were transferred to fresh Magenta GA-7 boxes containing Brite-Kote aluminum screen suspended over 50 mL of BDN, with two plants per box. The plants were incubated at 28°C with a 16 h light period for 9 weeks, changing the BDN after 8 weeks. Prior to inoculation, the plants were starved of nitrogen by replacing BDN medium with BD (nitrogen-free) medium and grown for two weeks.

Frankia sp. strain Eun1f was grown in MPN with 20 mM fructose at 28°C; every few weeks the cells were harvested and sub-cultured in fresh medium, and a homogenization step was included whenever hyphae formed large clumps. Eun1f was sub-cultured without homogenizing two weeks before plant inoculations. *Streptomyces* sp. (24) was grown from a glycerol stock for 9 days in liquid Czapek plus yeast extract at 28°C with shaking, then homogenized and subcultured in fresh Czapek plus yeast extract and grown an additional 5 days before inoculations. Bacterial cultures were pelleted, washed in sterile deionized water followed by sterile BD medium, and resuspended in sterile BD, adjusting the concentration to an optical density of 0.2 for *Streptomyces* and 0.6 for EuN1f. The plants were inoculated with 40-45 mL fresh BD with 5 mL Streptomyces and/or *Frankia* EuN1f suspension, for a total of 50 mL BD with *Streptomyces* at OD 0.02, EuN1f at OD 0.06, or both. Uninoculated negative control plants received 50 mL fresh BD only. Boxes were classified based on plant size and distributed such that each treatment received a similar set of three replicate boxes. The plants were incubated at 28°C with a 16 h light period for several weeks. Plants were monitored for nodule development, growth, and health.

No nodules were observed on either singly inoculated or co-inoculated plants. Plants exhibited signs of stress and nutrient deficiency, particularly severe chlorosis, red-tinted stems, and poor growth. These observations suggest that *A. glutinosa* is not capable of forming nodules with *Frankia* sp. EuN1f, and that *Streptomyces* sp. 24 does not induce nodulation of *A. glutinosa* with this *Frankia* strain outside its normal host range. However, it is important to note that the plants had already been subjected to

nutrient stress conditions prior to nitrogen starvation due to a long growth period (8 weeks) without replacing the BDN medium, and additional non-nitrogen nutrient stress conditions occurred after inoculation, as the BD medium was never replaced. It is possible that the stress was excessive enough to impair symbiotic capacity in the plants. Additionally, the EuN1f culture used in this experiment mistakenly underwent excessive centrifugation (1 hr 47 min instead of 20 min.) during sub-culture two weeks prior to inoculations, so there is a possibility that the culture was not viable. This experiment would need to be repeated to verify results.

Ridgway, K. P., Marland, L. A., Harrison, A. F., Wright, J., Young, J. P. W., & Fitter, A. H. (2004). Molecular diversity of Frankia in root nodules of Alnus incana grown with inoculum from polluted urban soils. *FEMS microbiology ecology*, *50*(3), 255-263.

Bosco, M., Fernandez, M. P., Simonet, P., Materassi, R., & Normand, P. (1992). Evidence that some Frankia sp. strains are able to cross boundaries between Alnus and Elaeagnus host specificity groups. *Applied and environmental microbiology*, *58*(5), 1569-1576.

Mansour, S., Swanson, E., Pesce, C., Simpson, S., Morris, K., Thomas, W. K., & Tisa, L. S. (2020). Draft genome sequences for the Frankia sp. strains CgS1, CcI156 and CgMI4, nitrogen-fixing bacteria isolated from Casuarina sp. in Egypt. *Journal of genomics*, *8*, 84.

antiSMASH analysis

12 *Herbaspirillum*

24 *Streptomyces*

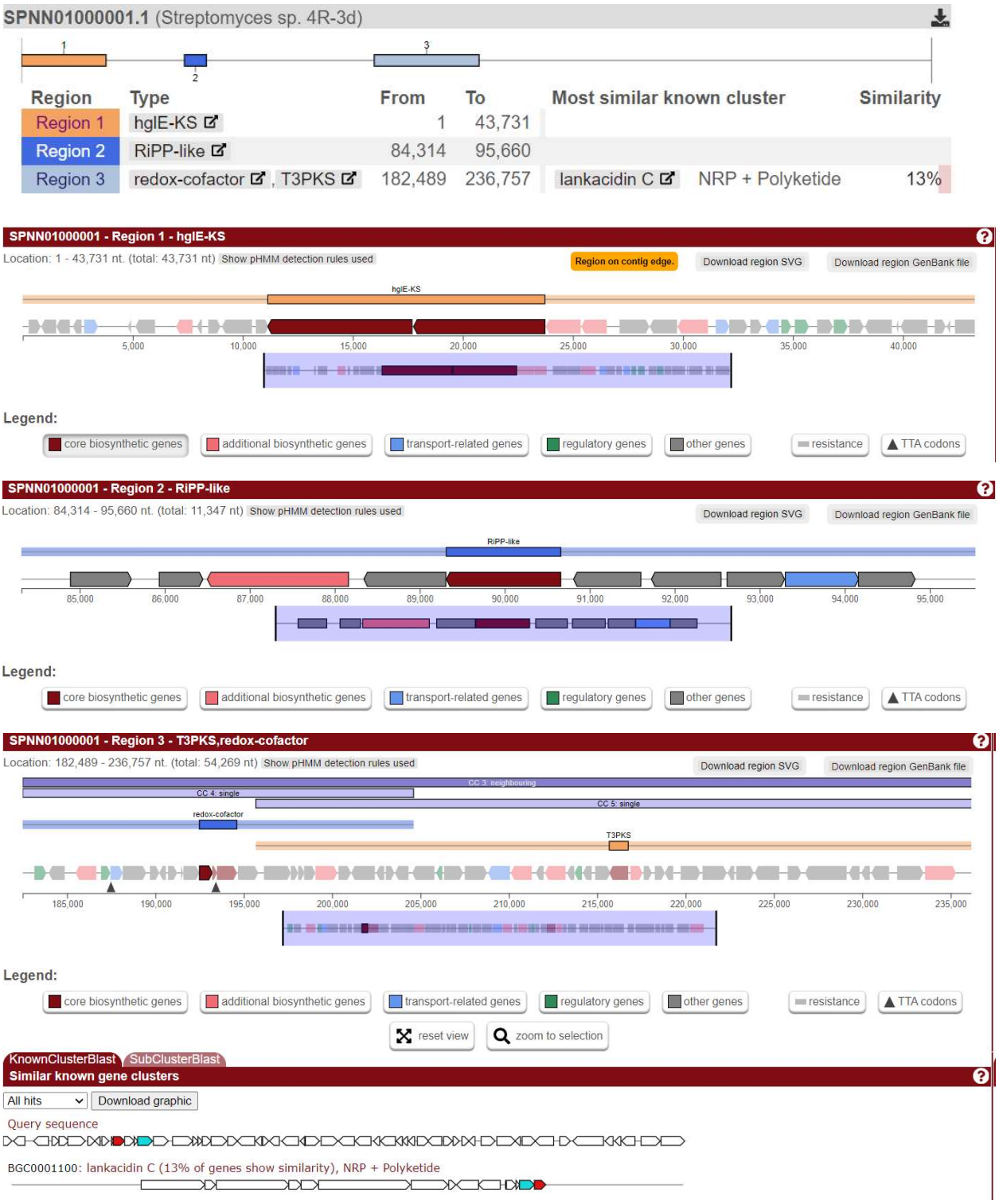

9 *Rhodococcus*

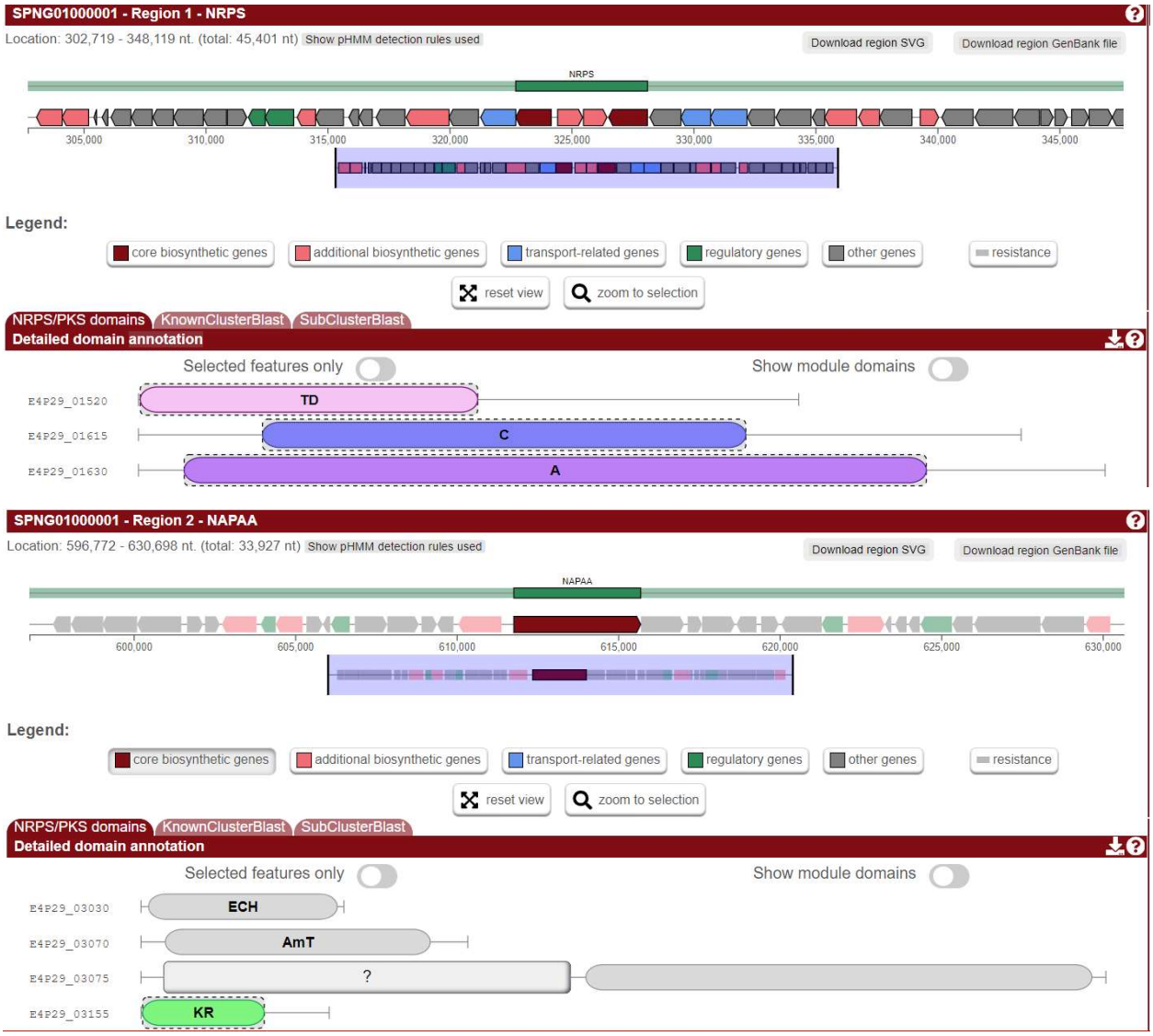
SPNG01000001 - Region 1 - NRPS
Location: 302,719 - 348,119 nt. (total: 45,401 nt)
Show pHMM detection rules used
Download region SVG
Download region GenBank file
NRPS
305,000
310,000
315,000
320,000
325,000
330,000
335,000
340,000
345,000
Legend:
core biosynthetic genes
additional biosynthetic genes
transport-related genes
regulatory genes
other genes
resistance
reset view
zoom to selection
NRPS/PKS domains
KnownClusterBlast
SubClusterBlast
Detailed domain annotation
Selected features only
Show module domains
E4P29_01520
TD
E4P29_01615
C
E4P29_01630
A
SPNG01000001 - Region 2 - NAPAA
Location: 596,772 - 630,698 nt. (total: 33,927 nt)
Show pHMM detection rules used
Download region SVG
Download region GenBank file
NAPAA
600,000
605,000
610,000
615,000
620,000
625,000
630,000
Legend:
core biosynthetic genes
additional biosynthetic genes
transport-related genes
regulatory genes
other genes
resistance
reset view
zoom to selection
NRPS/PKS domains
KnownClusterBlast
SubClusterBlast
Detailed domain annotation
Selected features only
Show module domains
E4P29_03030
ECH
E4P29_03070
AmT
E4P29_03075
?
E4P29_03155
KR